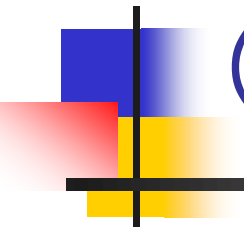
Optimal Spectral Decomposition in Ocean Analysis and Prediction

Peter C Chu
Naval Postgraduate School
Monterey, CA 93943
pcchu@nps.edu
https://www.nps.edu/pcchu

Utrecht University, Utrecht, The Netherlands, 22 April 2005

Collaborators

- Leonid Ivanov, Tanya Margolina, Oleg Melcheniko, Yuri. Poberezhny, Marine Hydrophysical Institute, Sevastopol, Ukraine
- Chenwu Fan, Naval Postgraduate School
- Lashmi Kantha, University of Colorado at Boulder
- Catherine Nicolis, Royal Meteorological Institute of Belgium



Part-1 Optimal Spectral Decomposition (OSD)

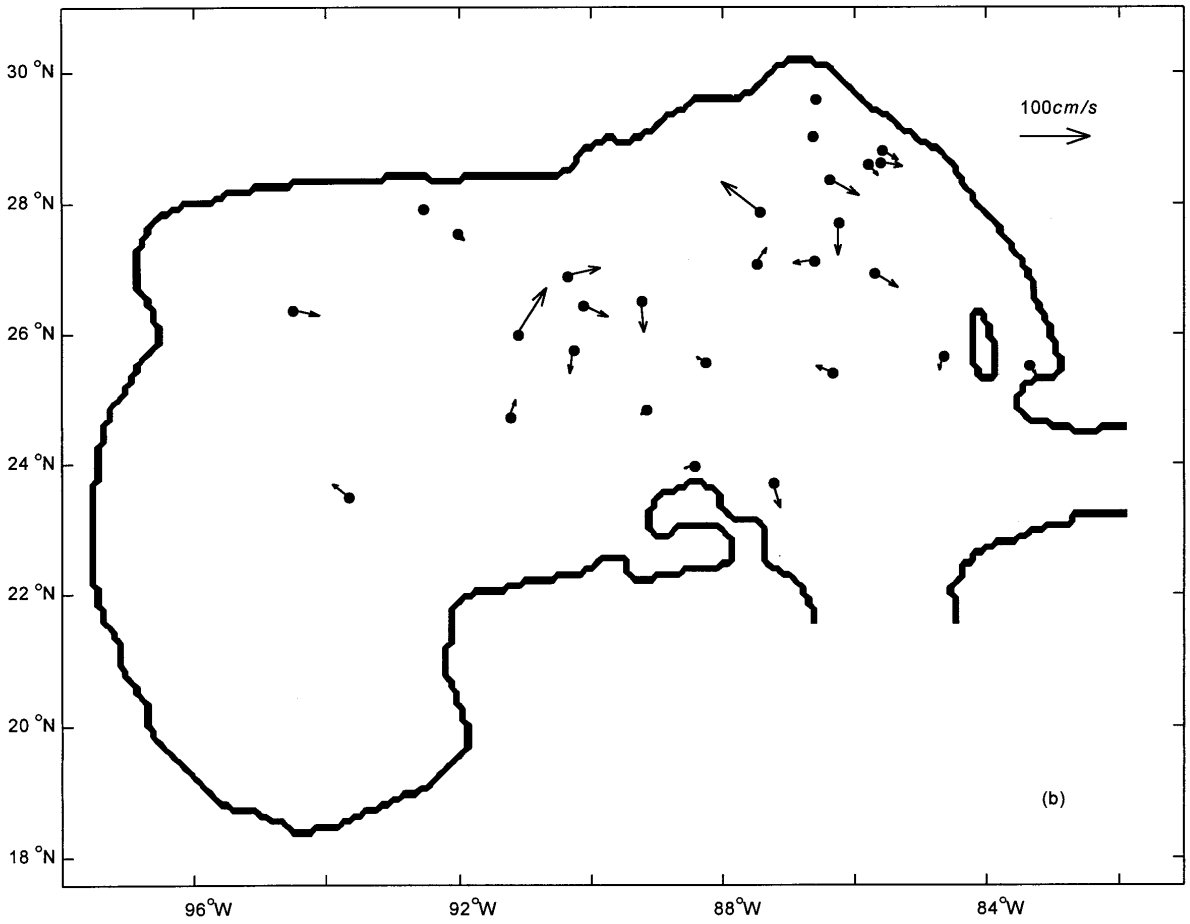
References

- Chu, P.C., L.M. Ivanov, T.P. Korzhova, T.M. Margolina, and O.M. Melnichenko, 2003a: Analysis of sparse and noisy ocean current data using flow decomposition. Part 1: Theory. Journal of Atmospheric and Oceanic Technology, 20 (4), 478-491.

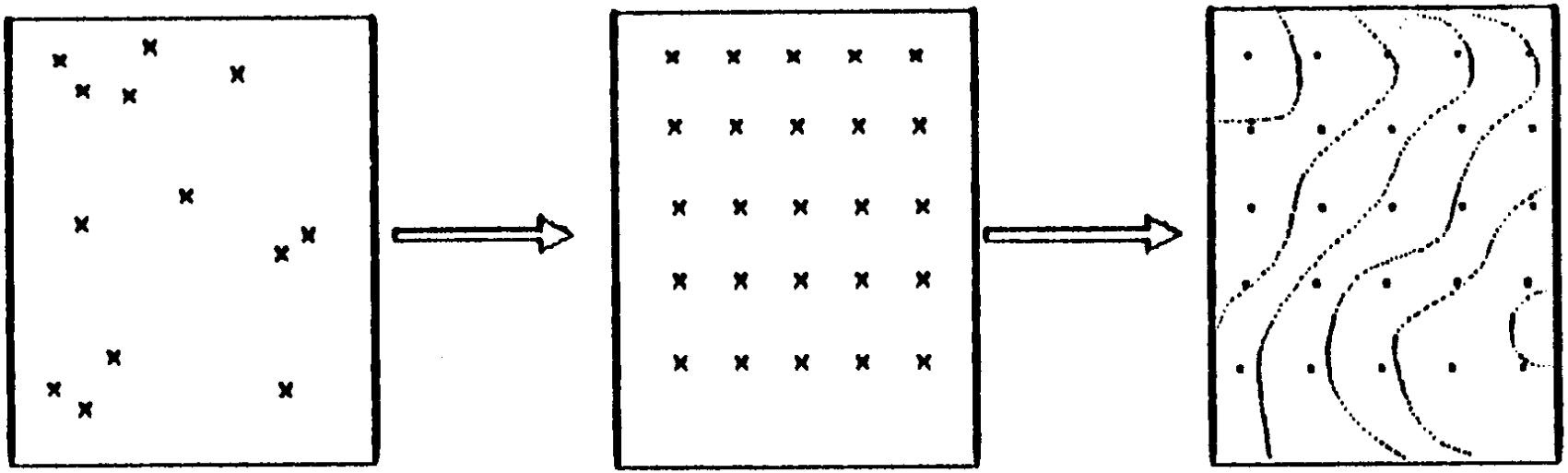
- Chu, P.C., L.M. Ivanov, T.P. Korzhova, T.M. Margolina, and O.M. Melnichenko, 2003b: Analysis of sparse and noisy ocean current data using flow decomposition. Part 2: Application to Eulerian and Lagrangian data. Journal of Atmospheric and Oceanic Technology, 20 (4), 492-512.

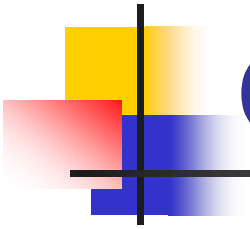
- Chu, P.C., L.M. Ivanov, and T.M. Margolina, 2004: Rotation method for reconstructing process and field from imperfect data. International Journal of Bifurcation and Chaos, in press.

Observational Data (Sparse and Noisy)



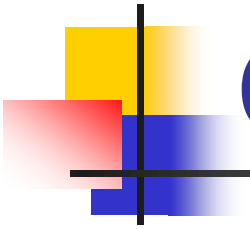
Most Popular Method for Ocean Data Analysis: Optimum Interpolation (OI)





OI Method Requires:

- (1) First guess field
- (2) Autocorrelation functions



Ocean velocity data

- (1) First guess field (?)
- (2) Unknown autocorrelation function

Davis (2002, 2004) Use of Numerical Model

- First-Guess Field
- Auto-Correlation Scale
- Mid-Depth Circulations of Pacific and Indian Oceans

Spectral Representation
An Alternative Method

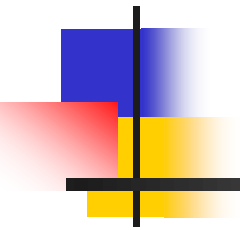
$$c(\mathbf{x}, z_k, t) = A_0(z_k, t) + \sum_{m=1}^{M} A_m(z_k, t)\ \Psi_m(\mathbf{x}, z_k),$$

Spatial Variability is represented by the basis functions

Two approaches to obtain basis functions

- EOFs
- Eigenfunctions of Laplace Operator

$$\nabla_h^2 \Psi_m = -\lambda_m \Psi_m, \quad \Psi_m|_\Gamma = 0, \quad m = 1, 2, \ldots, M$$



Spectral Representation for Velocity

Flow Decomposition

- 2 D Flow (Helmholtz), (Eremeev et al., 1992a, b)

$$\mathbf{u}_H = \mathbf{r} \times \nabla_H A_1 + \nabla_H A_3$$

- 3D Flow (Toroidal & Poloidal), Popular in Astrophysics (Chu et al., 2003a,b)

$$\mathbf{u} = \mathbf{r} \times \nabla A_1 + \mathbf{r} A_2 + \nabla A_3$$

3D Incompressible Flow

- When

$$\nabla \cdot \mathbf{u} = 0$$

- We have

$$\mathbf{u} = \nabla \times (\mathbf{r}\Psi) + \nabla \times \nabla \times (\mathbf{r}\Phi) .$$

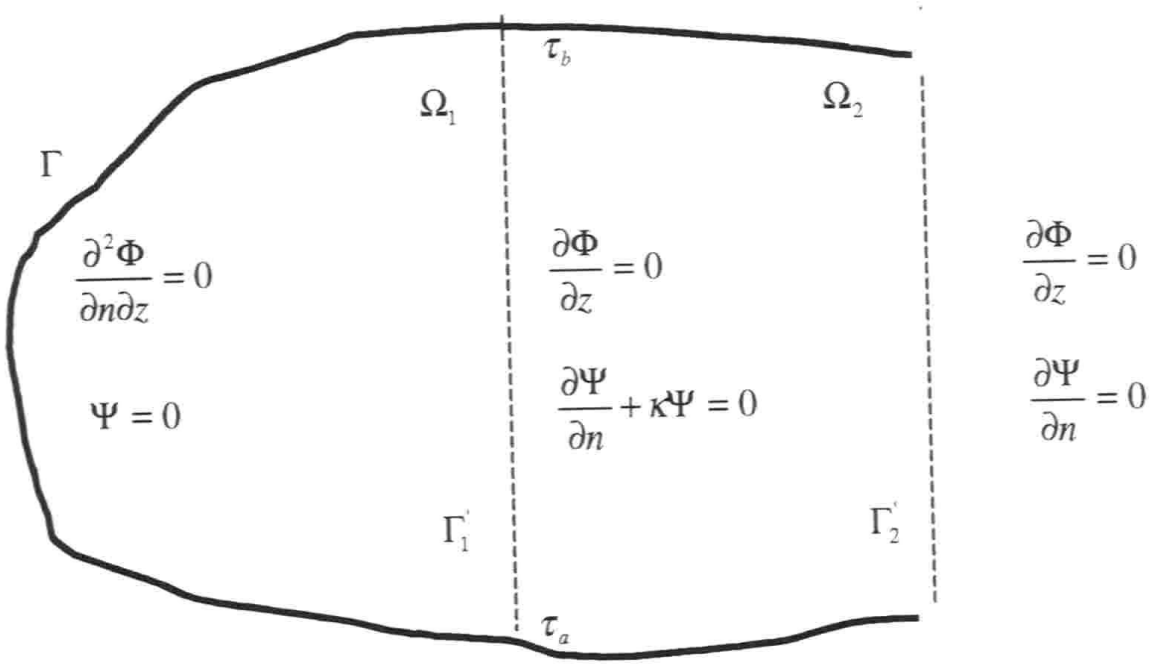
3D Flow Decomposition

$$u = \frac{\partial \Psi}{\partial y} + \frac{\partial^2 \Phi}{\partial x \partial z}, \qquad v = -\frac{\partial \Psi}{\partial x} + \frac{\partial^2 \Phi}{\partial y \partial z},$$

- $$\triangle \Psi = -\zeta$$

$$\triangle \Phi = -w$$

Boundary Conditions



Basis Functions (Closed Basin)

$$\triangle \Psi_k = -\lambda_k \Psi_k, \quad \Psi_k|_\Gamma = 0, \qquad k = 1, \ldots, \infty$$

$$\triangle \Phi_m = -\mu_m \Phi_m, \quad \frac{\partial \Phi_m}{\partial n}|_\Gamma = 0, \qquad m = 1, \ldots, \infty.$$

Basis Functions (Open Boundaries)

$$\triangle \Psi_k = -\lambda_k \Psi_k,$$

$$\triangle \Phi_m = -\mu_m \Phi_m,$$

$$\Psi_k|_\Gamma = 0, \quad \frac{\partial \Phi_m}{\partial n}|_\Gamma = 0,$$

$$\left[\frac{\partial \Psi_k}{\partial n} + \kappa(\tau)\Psi_k\right]|_{\Gamma_1'} = 0, \quad \Phi_m|_{\Gamma_1'} = 0,$$

Spectral Decomposition

$$u_{KM} = \sum_{k=1}^{K} a_k(z,t^\circ)\frac{\partial \Psi_k(x,y,z,\kappa^\circ)}{\partial y} + \sum_{m=1}^{M} b_m(z,t^\circ)\frac{\partial \Phi_m(x,y,z)}{\partial x},$$

$$v_{KM} = -\sum_{k=1}^{K} a_k(z,t^\circ)\frac{\partial \Psi_k(x,y,z,\kappa^\circ)}{\partial x} + \sum_{m=1}^{M} b_m(z,t^\circ)\frac{\partial \Phi_m(x,y,z)}{\partial y}$$

Optimal Mode Truncation

$$J(a_{1,\dots,}a_K, b_{1,\dots,}b_M, \kappa, P) = \frac{1}{2}\left(\left\|u_p^{obs} - u_{KM}\right\|_P^2 + \left\|v_p^{obs} - v_{KM}\right\|_P^2\right) \to \min,$$

Vapnik (1983) Cost Function

$$J_{emp} = J(a_{1,\ldots,}a_K, b_{1,\ldots,}b_M, \kappa, P).$$

$$\text{Prob}\left\{ \sup_{K,M,S} |\langle J(K,M,S)\rangle - J_{emp}(K,M,S)| \geq \mu \right\} \leq g(P,\mu)$$

$$\lim_{P\to\infty} g(P,\mu) = 0$$

Optimal Truncation

- ARGO Data (Mid-Depth North Atlantic)

  $K_{opt} = 38$, $M_{opt} = 24$

- Gulf of Mexico, Monterey Bay, Louisiana-Texas Shelf

  $K_{opt} = 40$, $M_{opt} = 30$

Determination of Spectral Coefficients (Ill-Posed Algebraic Equation)

$$\mathbf{A}\hat{\mathbf{a}} = \mathbf{QY},$$

Rotation Method (Chu et al., 2004)

$$\mathbf{SA}\,\hat{\mathbf{a}} = \mathbf{SQY},$$

$$J_1 = \|\mathbf{A}\|^2 - \frac{\|\mathbf{SQY}\|^2}{\|\mathbf{a}\|^2} \rightarrow \max,$$

Part-2 Application in Ocean Data Analysis

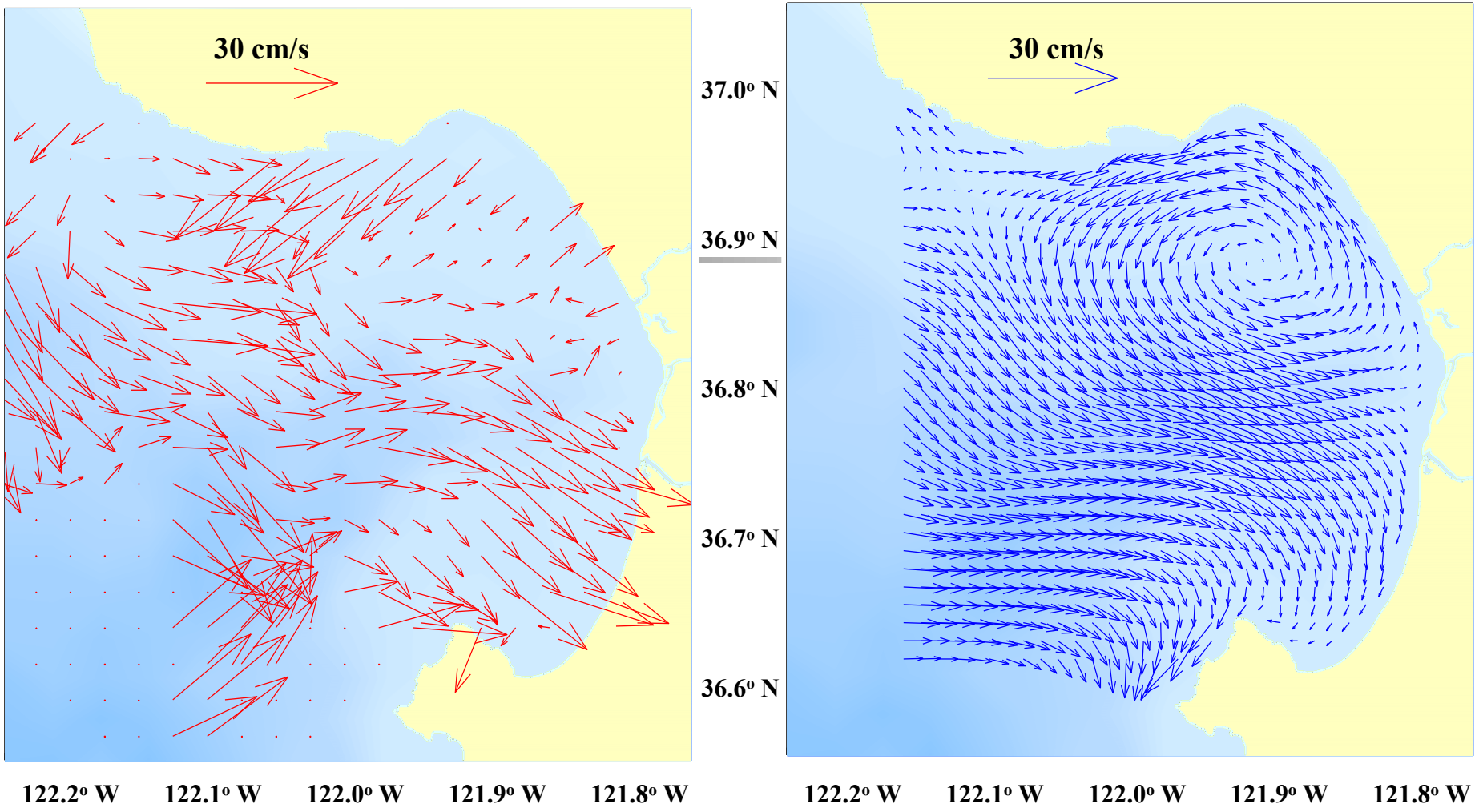
- CODAR (Monterey Bay)
- ARGO Floats (Mid-Depth Atlantic Circulation)
- Combined Current Meters and Drifters (LATEX)

Example 1- CODAR Data Analysis



Monterey Bay

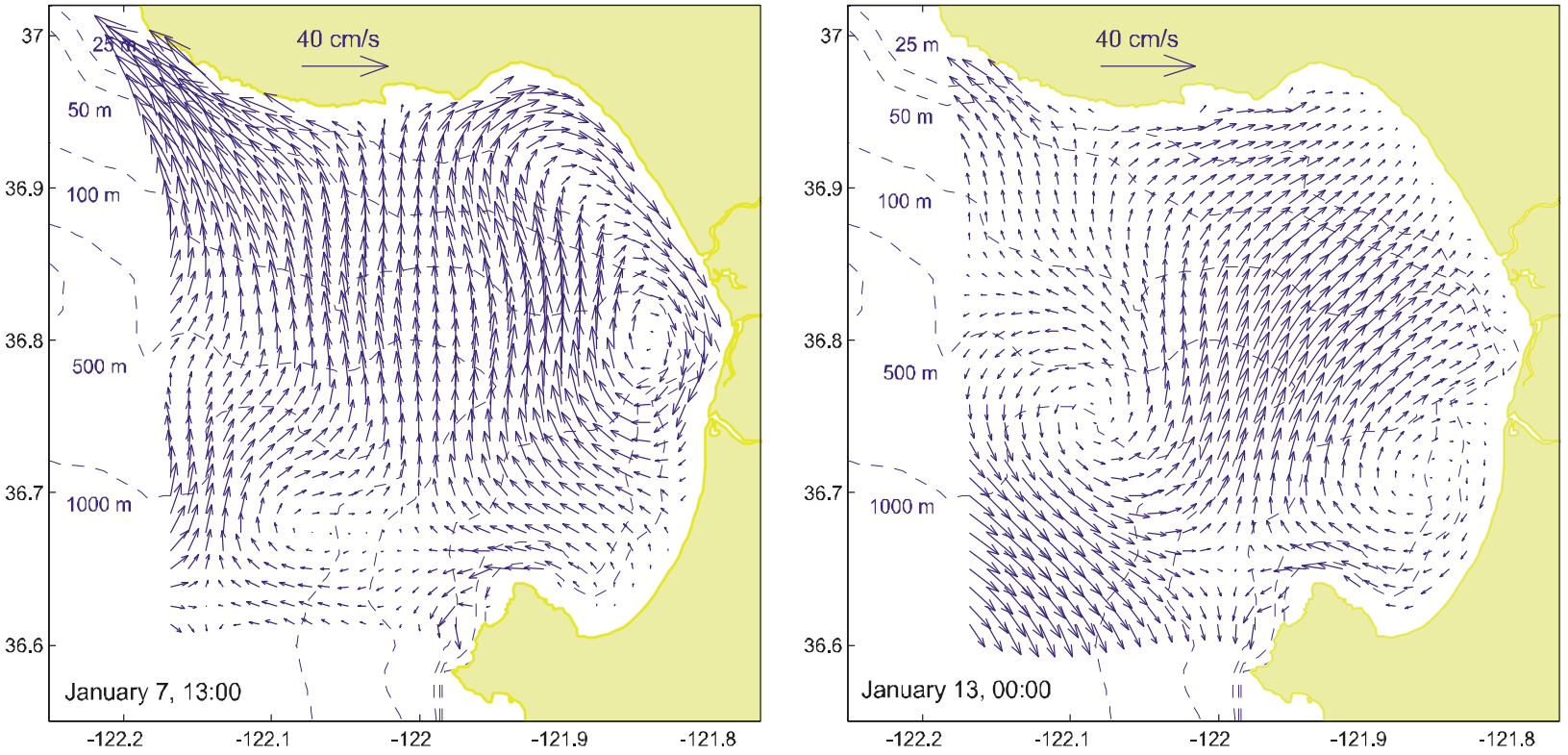




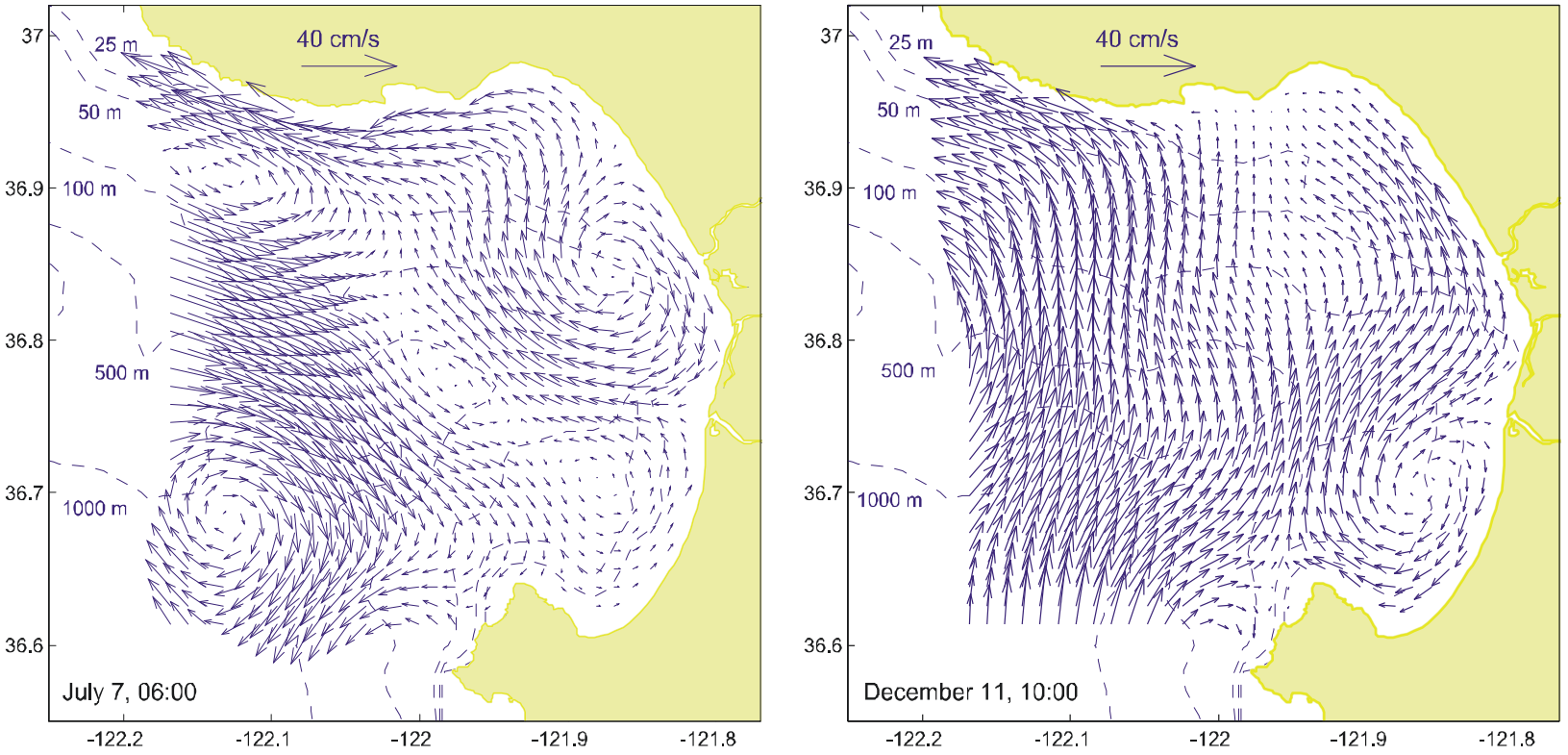
Place for comments: left - radar derived currents for 17:00 UT December 1, 1999

right – reconstructed velocity field.

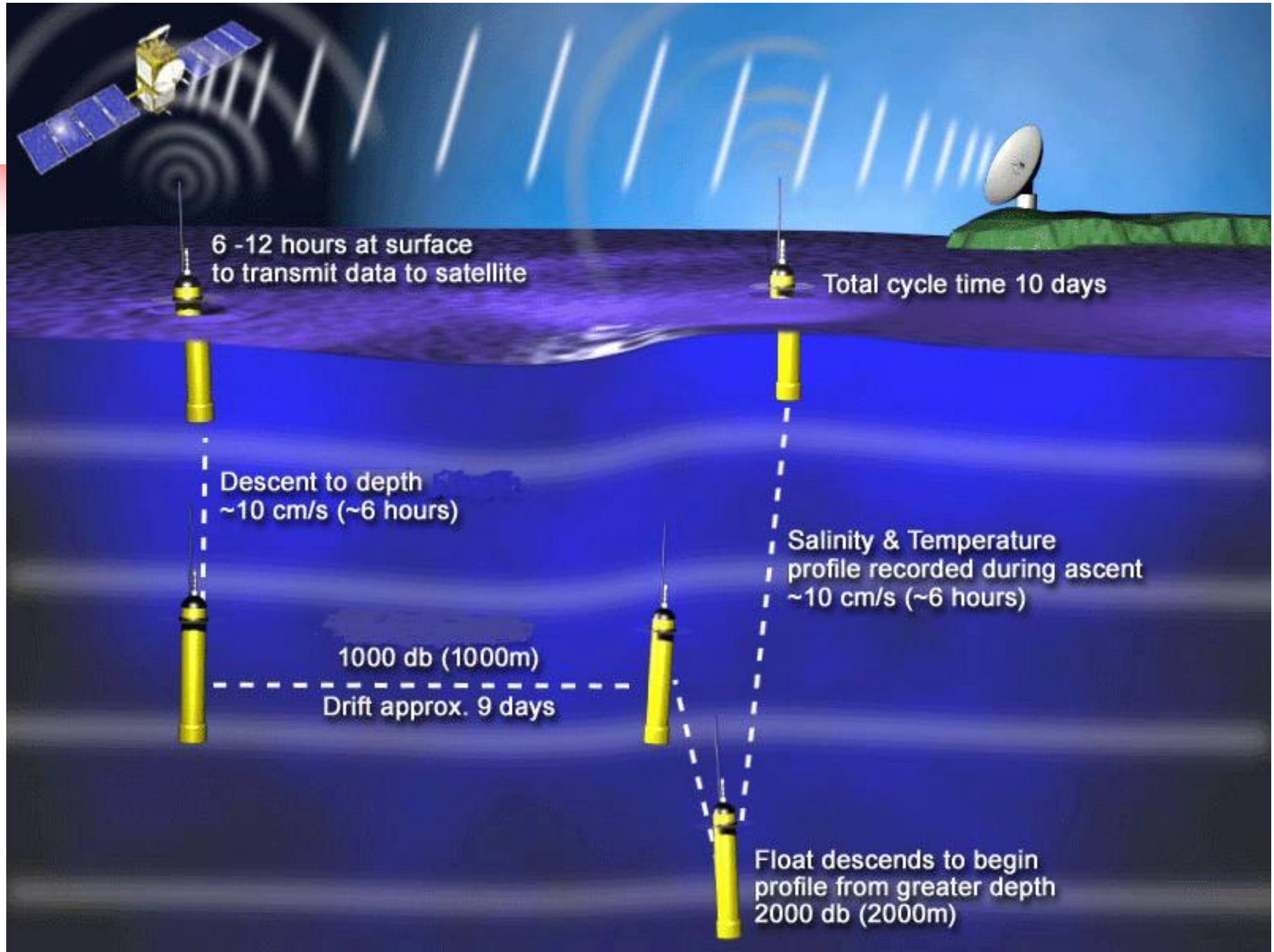
Temporally Varying Surface Circulation



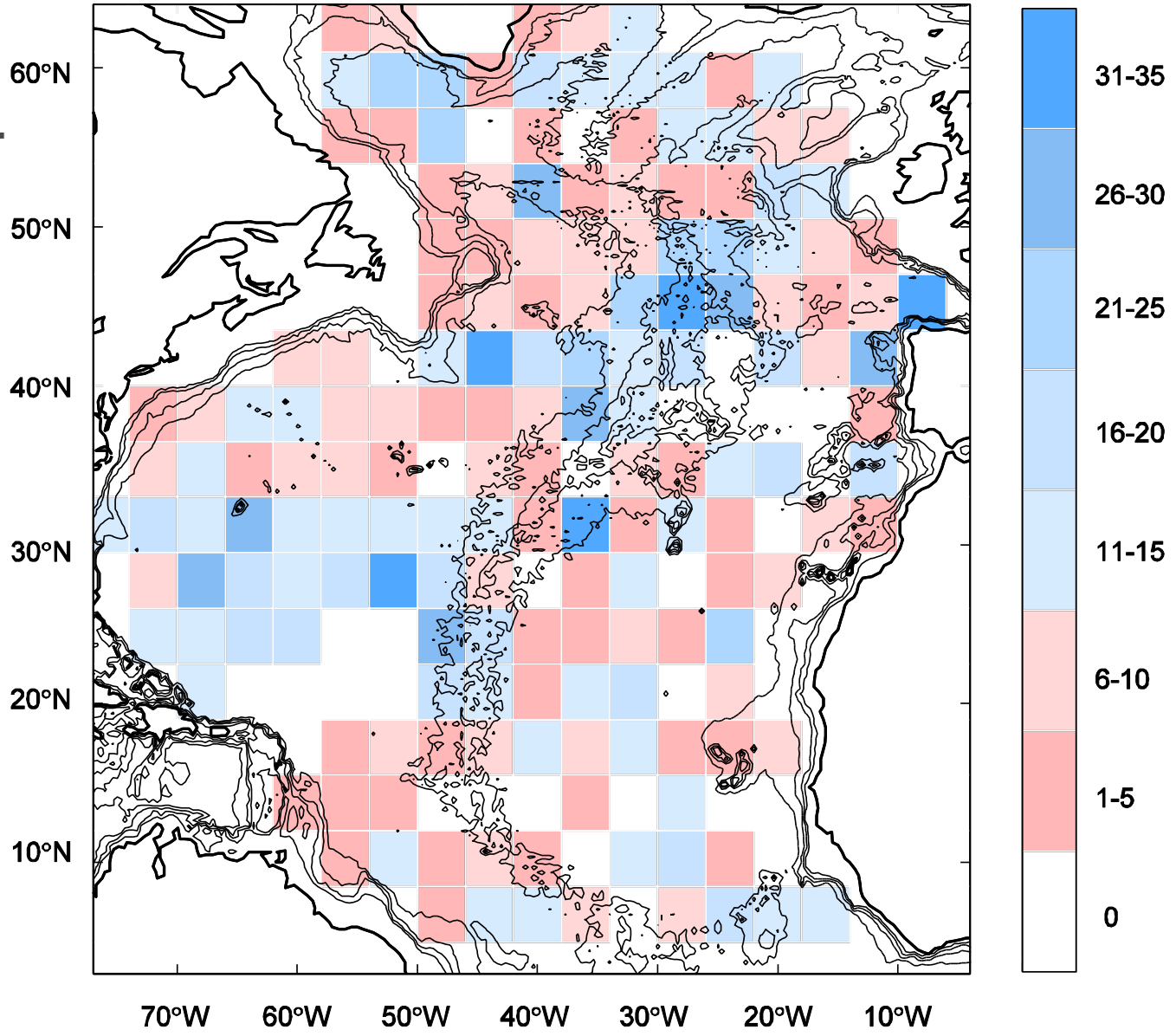
Temporally Varying Surface Circulation



Example 2 Mid-depth (1000 m) North Atlantic Circulation identified from ARGO Data

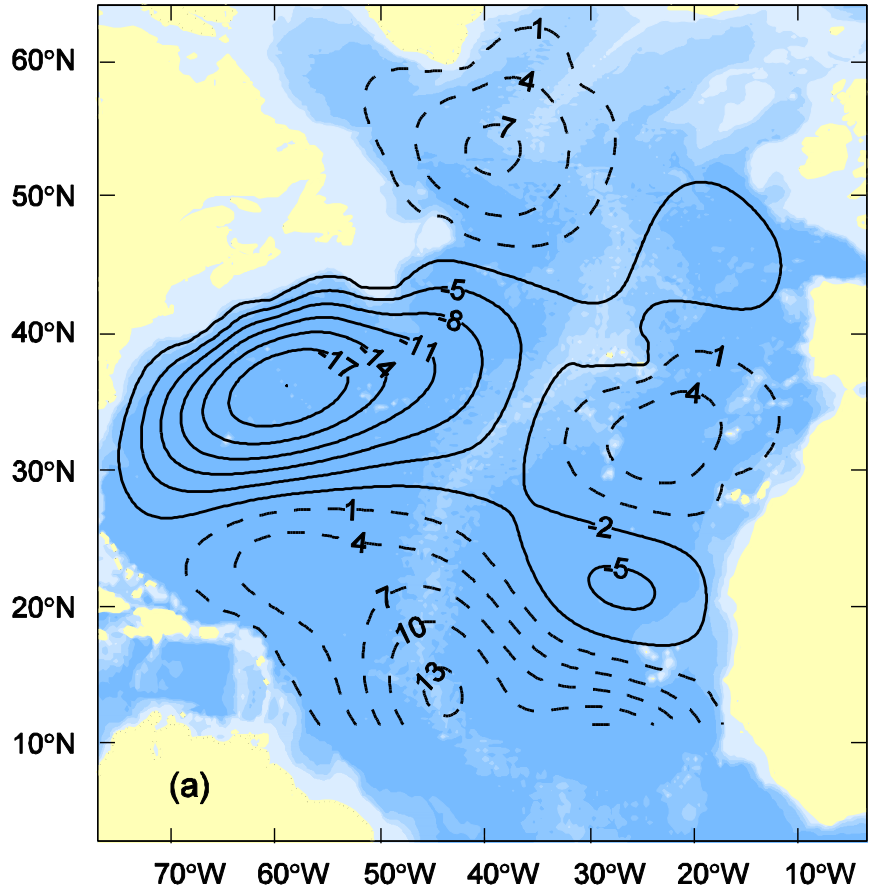

6 -12 hours at surface
to transmit data to satellite
Total cycle time 10 days
Descent to depth
~10 cm/s (~6 hours)
Salinity & Temperature
profile recorded during ascent
~10 cm/s (~6 hours)
1000 db (1000m)
Drift approx. 9 days
Float descends to begin
profile from greater depth
2000 db (2000m)

ARGO Float Coverage (Aug-Dec 2004)

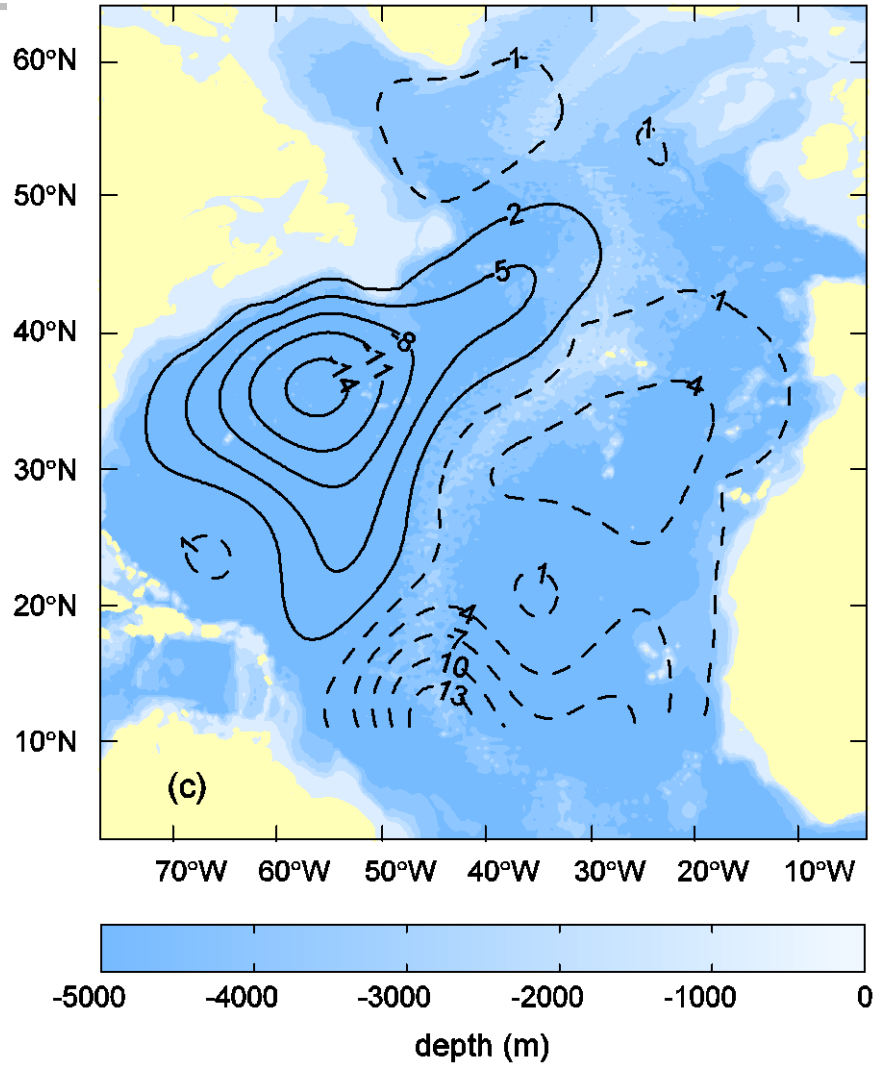


Streamfunction (10^3 m^2/s)

Mode-1
Dec03 – Mar04

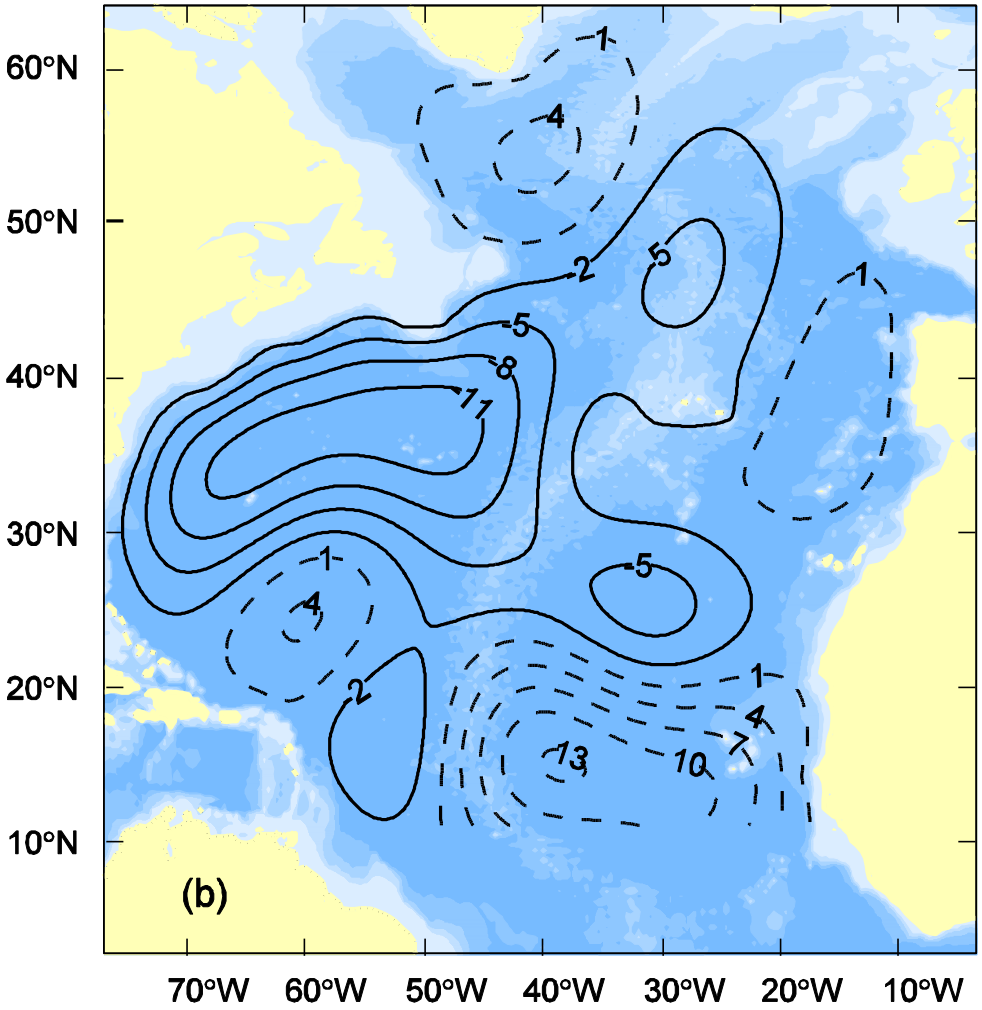


Mode-2
Aug-Dec04



Transition between two modes

Apr-Jul 2004



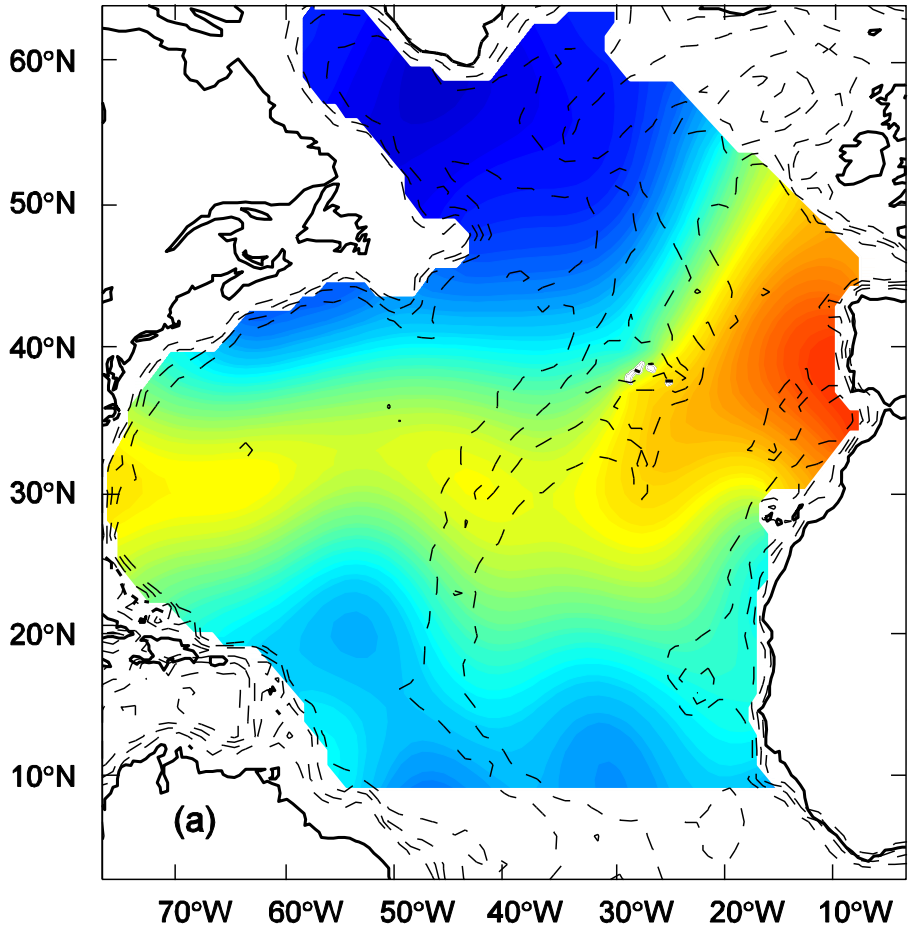
Bi-Modality Structure

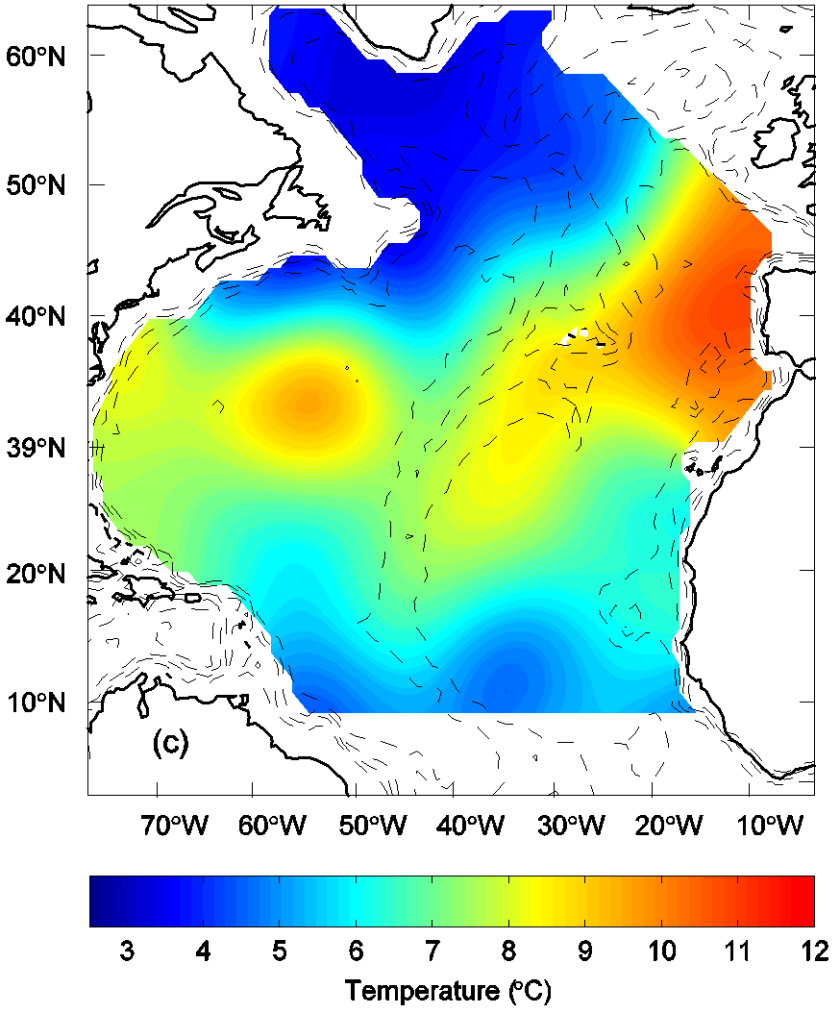
- Mode-1: Advection pathways to cross the mid-Atlantic Ridge
- Mode-2: No advection pathways
- Reid (1994) identified Mode-2 as the mid-depth north Atlantic Circulation pattern.

Temperature

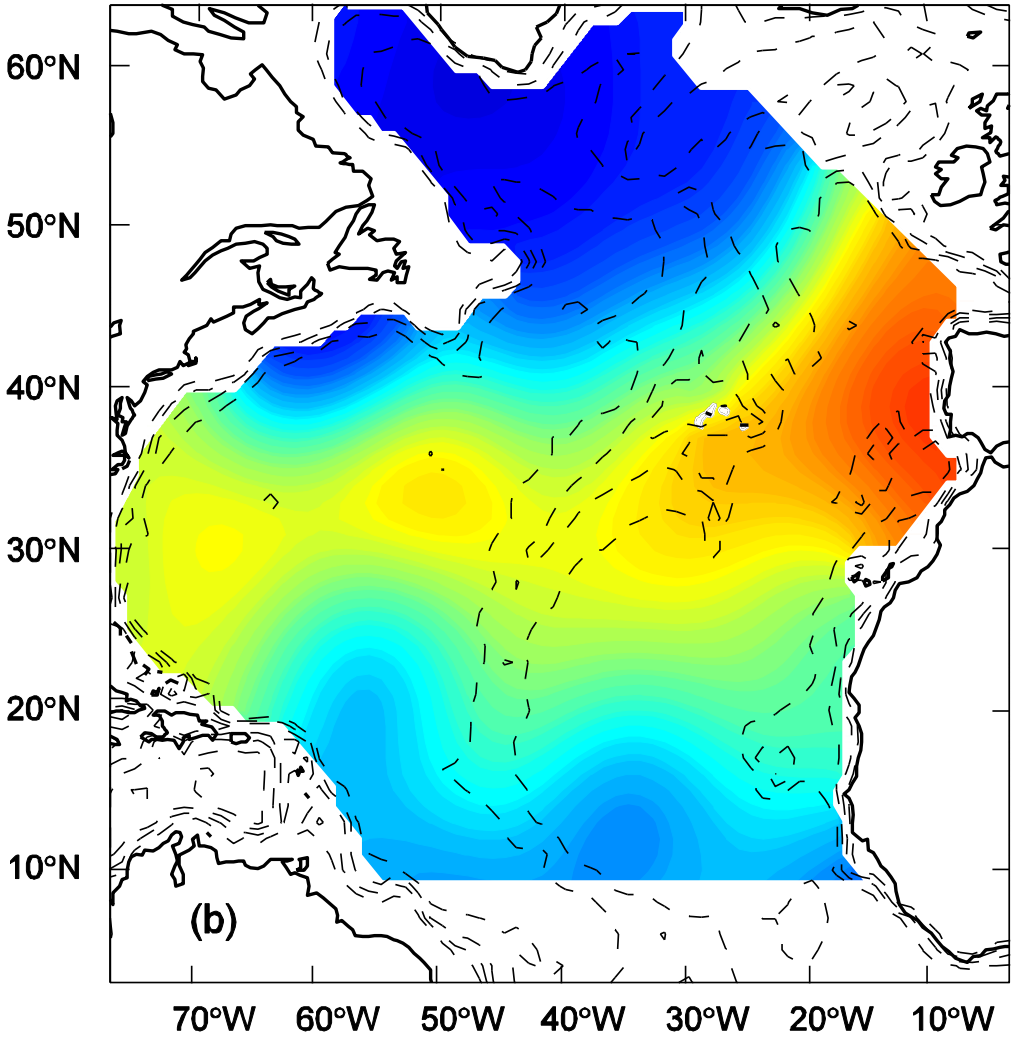
Feb 04 (Mode-1)

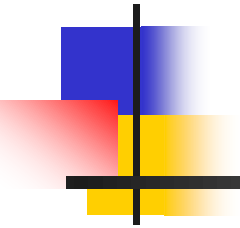
Dec04 (Mode-2)





Temperature, July 2004 (Transition)





Example 3

Current Reversal in Louisiana-Texas Continental Shelf (LTCS)

Reference

- Chu, P.C., L.M. Ivanov, and O.V. Melnichenko, 2005: Fall-winter current reversals on the Taxes-Lousiana continental shelf, Journal of Physical Oceanography, in press.

Ocean Velocity Data

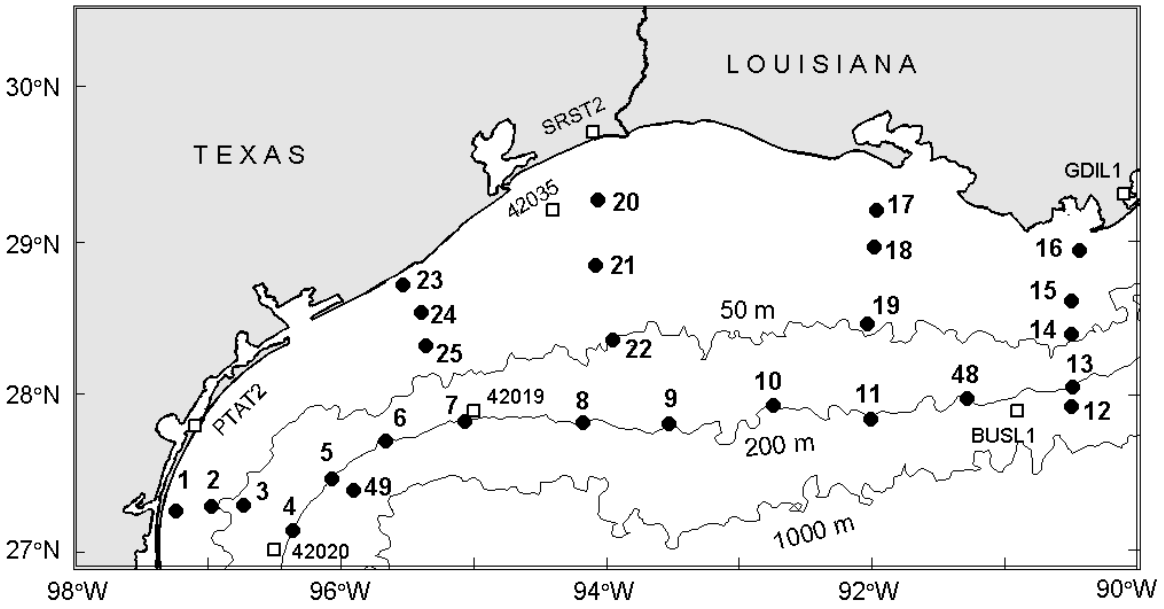
- 31 near-surface (10-14 m) current meter moorings during LATEX from April 1992 to November 1994

- Drifting buoys deployed at the first segment of the Surface Current and Lagrangian-drift Program (SCULP-I) from October 1993 to July 1994.

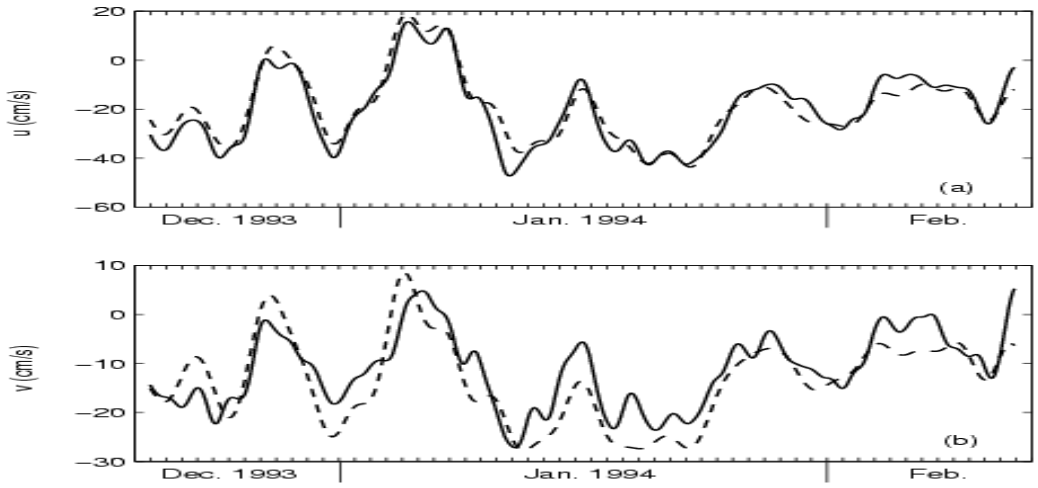
Surface Wind Data

- **7 buoys of the National Data Buoy Center (NDBC) and industry (C-MAN) around LATEX area**

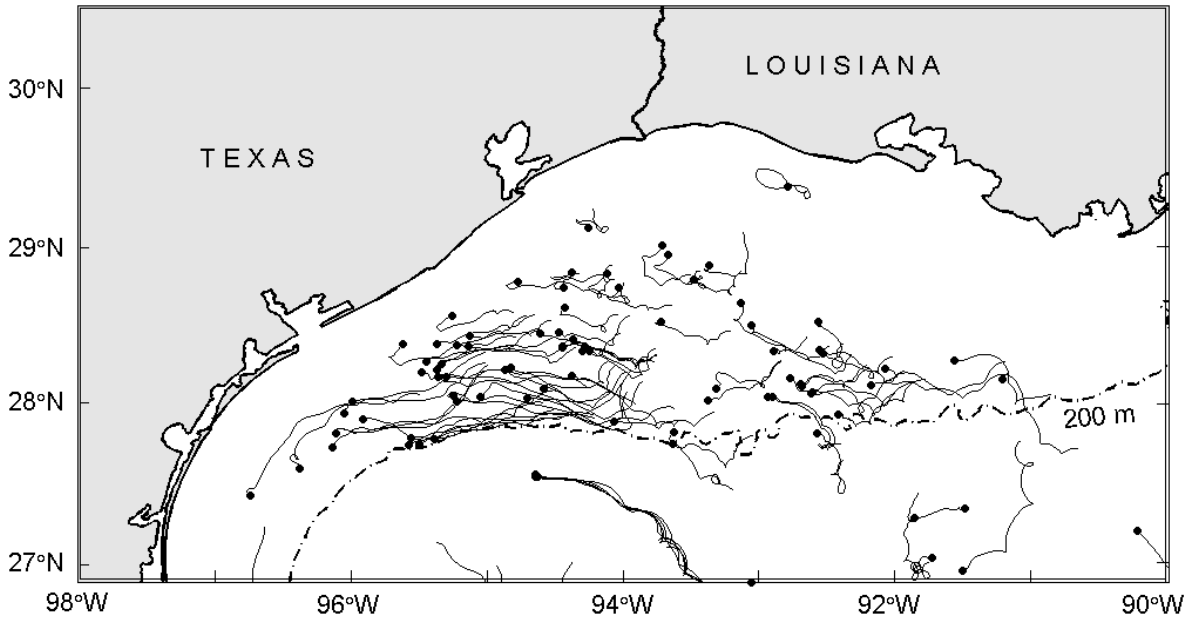
Moorings and Buoys



Reconstructed and observed circulations at Station-24.



LTCS current reversal detected from SCULP-I drift trajectories.



Probability of TLCS Current Reversal for Given Period (T)

- n_0 ~0-current reversal
- n_1~ 1-current reversal
- n_2~ 2-current reversals
- m ~ all realizations

$$P_0(T) = \frac{n_0}{m}, P_1(T) = \frac{n_1}{m}, P_2(T) = \frac{n_2}{m},$$

Fitting the Poison Distribution

$$P_k(T) = \frac{1}{k!}(\mu T)^k \exp(-\mu T)$$

$$k=0, 1, 2$$

μ is the mean number of reversal for a single time interval

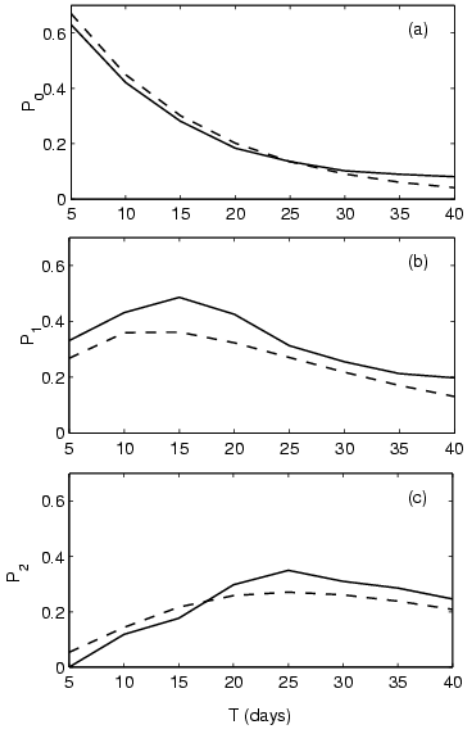
μ ~ 0.08

Dependence of P_0, P_1, P_2 on T

For observational periods larger than 20 days, the probability for no current reversal is less than 0.2.

For 15 day observational period, the probability for 1-reversal reaches 0.5

Data – Solid Curve
Poison Distribution Fitting – Dashed Curve



Time Interval between Successive Current Reversals (not a Rare Event)

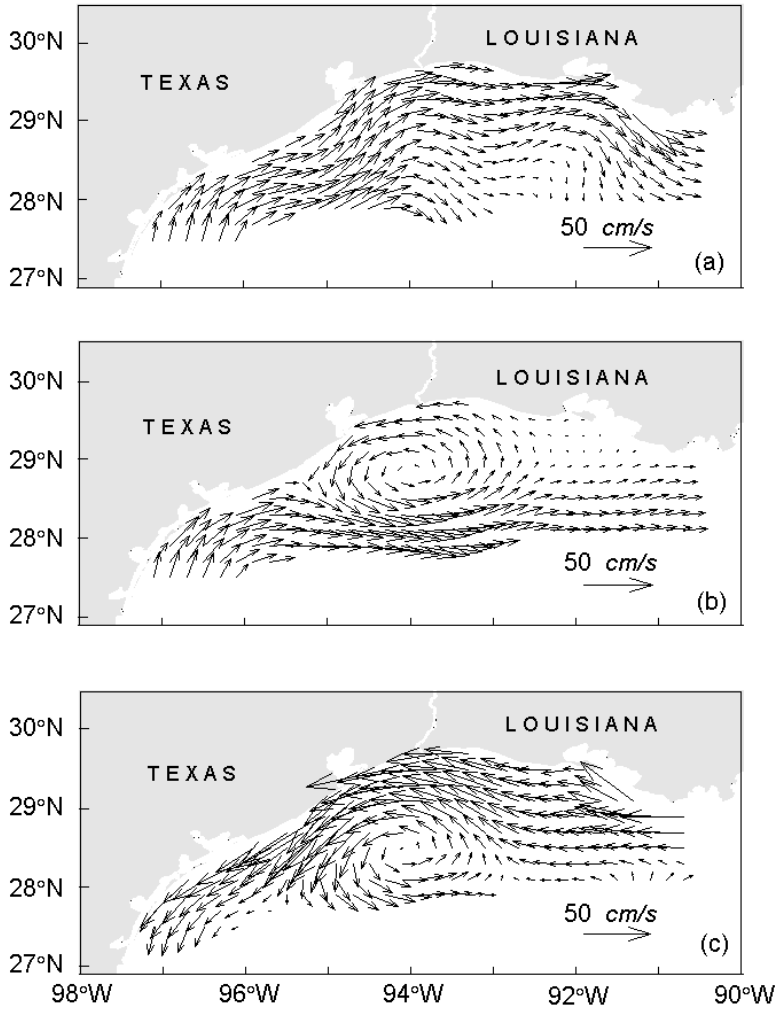
$$p(\tau) = \mu \exp(-\mu\tau)$$

LTCS current reversal detected from the reconstructed velocity data

December 30, 1993

January 3, 1994

January 6, 1994



EOF Analysis of the Reconstructed Velocity Filed

EOF	Variance (%)		
	01/21/93-05/21/93	12/19/93-04/17/94	10/05/94-11/29/94
1	80.2	77.1	74.4
2	10.1	9.5	9.3
3	3.9	5.6	6.9
4	1.4	3.3	4.6
5	1.1	1.4	2.3
6	0.7	1.1	0.8

Mean and First EOF Mode

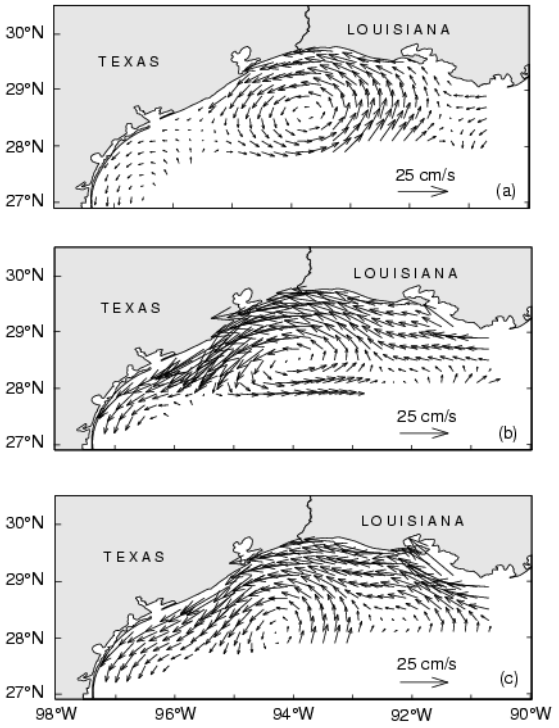
$$\tilde{\mathbf{u}}(x, y, t) = \overline{\mathbf{u}}(x, y) + A_1(t)\mathbf{u}_1(x, y),$$

Mean Circulation

1. First Period (01/21-05/21/93)

2. Second Period 12/19/93-04/17/94)

3. Third Period (10/05-11/29/94)

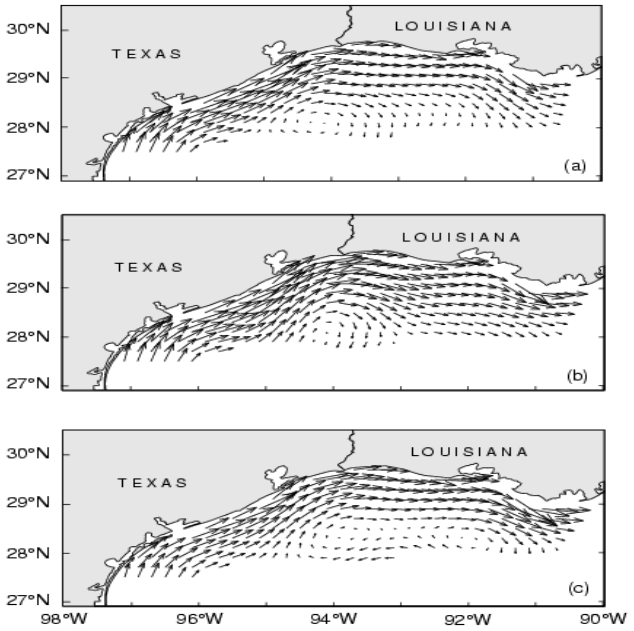


EOF1

1. First Period (01/21-05/21/93)

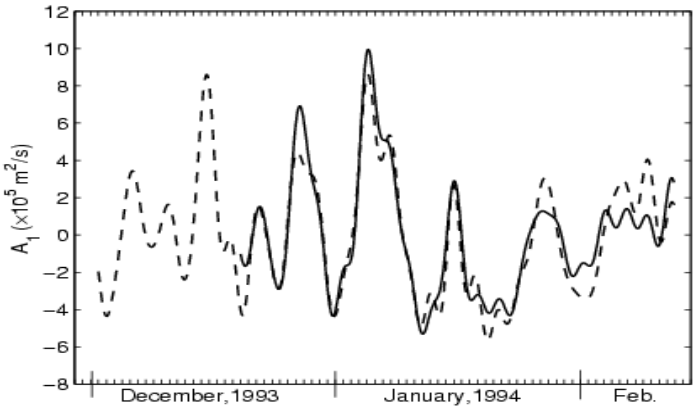
2. Second Period 12/19/93-04/17/94)

3. Third Period (10/05-11/29/94)



- Calculated $A_1(t)$

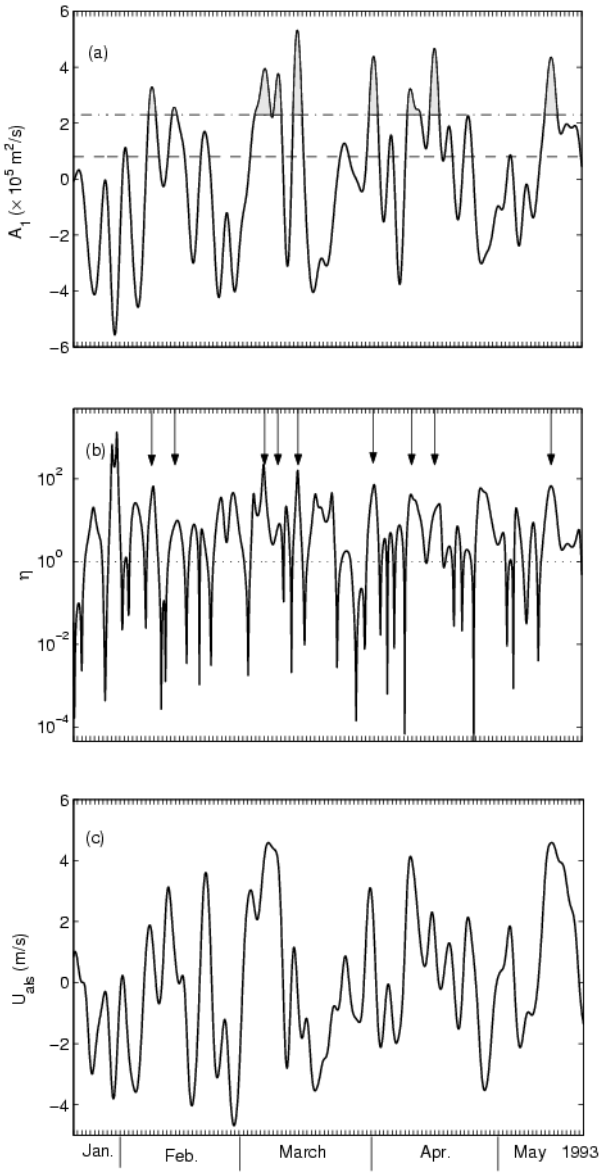
Using Current Meter Mooring (solid) and SCULP-1 Drifters (dashed)



- 8 total reversals observed

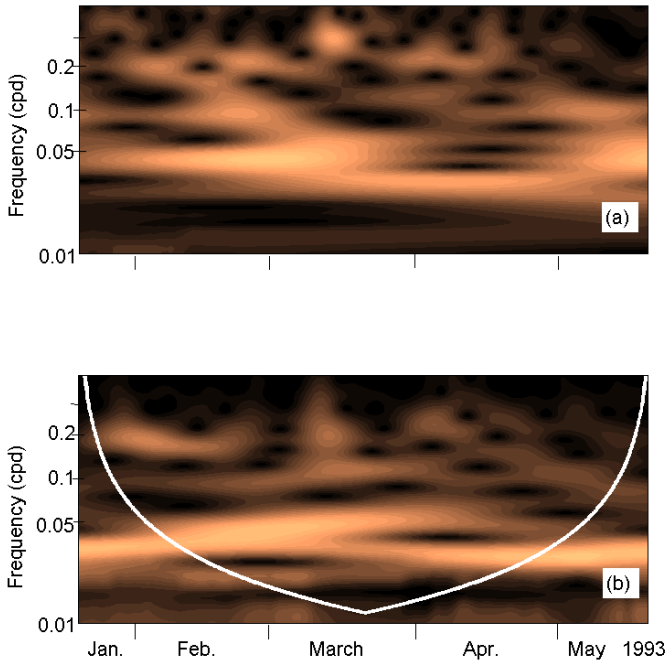
$$\eta = A_1^2 / \sum_{n=2}^{6} A_n^2$$

- U_{als} ~ alongshore wind



Morlet Wavelet

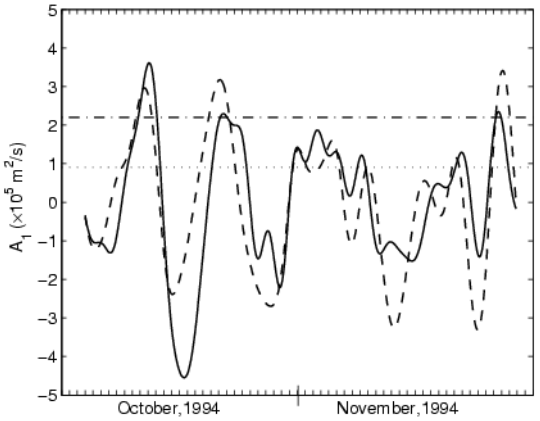
- $A_1(t)$
- U_{als}



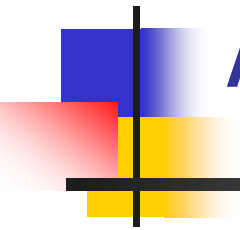
$$\Phi(t) = \pi^{-4} \exp(imt - t^2/2), \quad \mathrm{m} = 6$$

- Regression between
- $A_1(t)$ and Surface
- Winds

- Solid Curve (reconstructed)
- Dashed Curve (predicted using winds)



$$A_1(t) = \alpha\left[U(t) - \overline{U}\right] + \beta\left[V(t) - \overline{V}\right] + \gamma$$



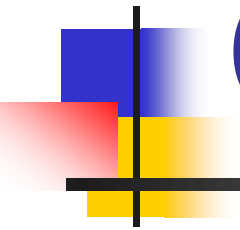
Part-3
Application in Modeling

This question should be answered before running any model

- How long is an ocean (or atmospheric) model valid once being integrated from its initial state?

References

- Chu, P.C., L.M. Ivanov, T. M. Margolina, and O.V. Melnichenko, On probabilistic stability of an atmospheric model to various amplitude perturbations. Journal of the Atmospheric Sciences, 59, 2860-2873.
- Chu, P.C., L.M. Ivanov, C.W. Fan, 2002: Backward Fokker-Planck equation for determining model valid prediction period. Journal of Geophysical Research, 107, C6, 10.1029/2001JC000879.
- Chu, P.C., L. Ivanov, L. Kantha, O. Melnichenko, and Y. Poberezhny, 2002: Power law decay in model predictability skill. Geophysical Research Letters, 29 (15), 10.1029/2002GLO14891.
- Chu, P.C., L.M. Ivanov, L.H. Kantha, T.M. Margolina, and O.M. Melnichenko, and Y.A, Poberenzhny, 2004: Lagrangian predictabilty of high-resolution regional ocean models. Nonlinear Processes in Geophysics, 11, 47-66.



(1) First-Passage Time

Physical Reality

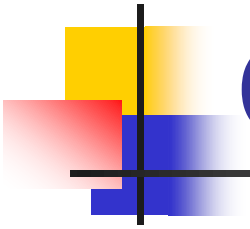
- $\boldsymbol{Y}$
- Physical Law: $d\boldsymbol{Y}/dt = \boldsymbol{h}(\boldsymbol{y}, t)$
- Initial Condition: $\boldsymbol{Y}(t_0) = \boldsymbol{Y}_0$

Atmospheric & Oceanic Models

- ***X*** is the prediction of **Y**
- $d\boldsymbol{X}/dt = \boldsymbol{f}(\boldsymbol{X}, t) + q(t)\,\boldsymbol{X}$
- Initial Condition: $\boldsymbol{X}(t_0) = \boldsymbol{X}_0$
- Stochastic Forcing:
- $\langle q(t) \rangle = 0$
- $\langle q(t)q(t') \rangle = q^2\delta(t-t')$

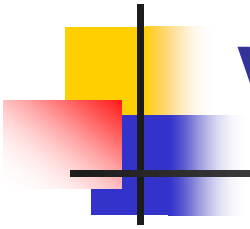
Model Error

- $Z = X - Y$
- Initial: $Z_0 = X_0 - Y_0$



One Missing Parameter

- Tolerance Level ε
- Maximum accepted error

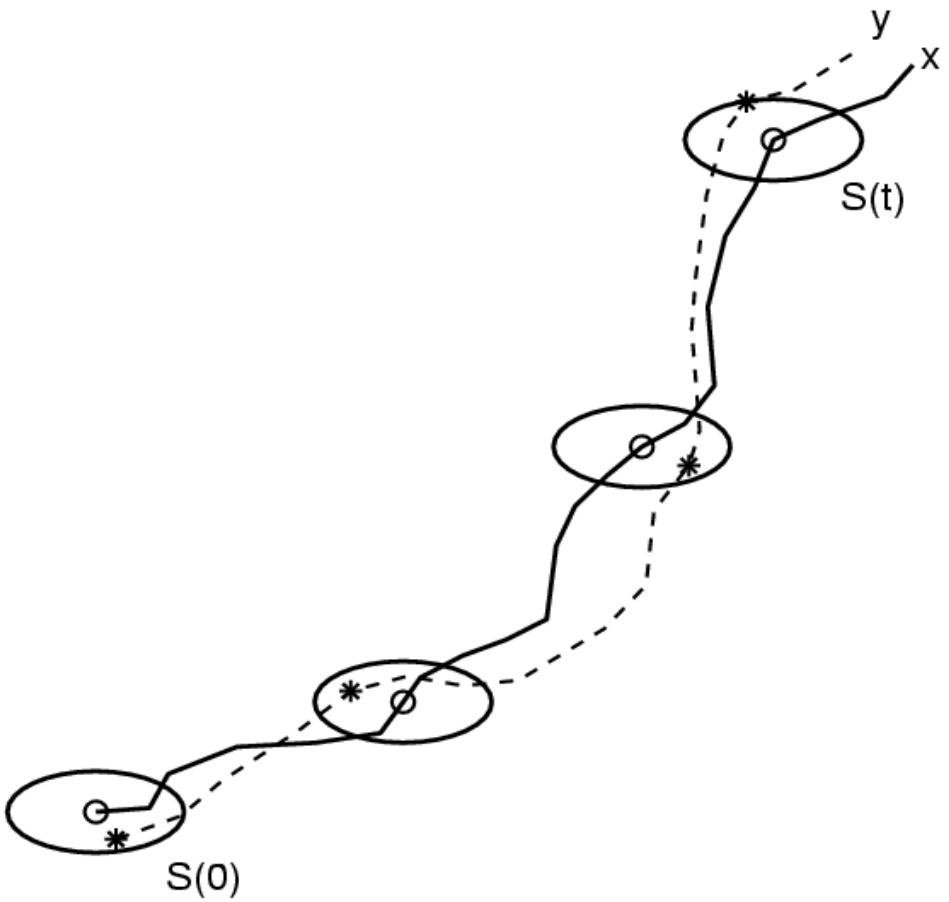


Valid Prediction Period

- VPP is defined as the time period when the prediction error first exceeds a pre-determined criterion (i.e., the tolerance level ε).

- VPP is the First-Passage Time

Valid Predict Period (VPP)



- VPP is defined as the time period when the prediction error first exceeds a pre-determined criterion (i.e., the tolerance level ε).

First-Passage Time



Conditional Probability Density Function

- Initial Error: z_0
- $(t - t_0)$? Random Variable
- Conditional PDF of $(t - t_0)$ with given z_0 ?
  - $P[(t - t_0) | z_0]$

Two Approaches

- Analytical (low dimension dynamical system)
- Practical (operational atmospheric or ocean model)

(2) Backward Fokker-Planck Equation

$$\frac{\partial P}{\partial t}-\sum_{i=1}^{J}\left(f_i-\frac{d\hat{x}_i}{dt}\right)\frac{\partial P}{\partial z_i^0}-\frac{1}{2}\sum_{i=1}^{J}\sum_{j=1}^{J}\sum_{l=1}^{J}k_{il}k_{lj}\frac{\partial^2 P}{\partial z_i^0\partial z_j^0}=0,$$

Moments

$$\tau_1(\mathbf{z}_0) = \int_{t_0}^{\infty} P(t_0, \mathbf{z}_0, t - t_0)(t - t_0)dt$$

$$\tau_2(\mathbf{z}_0) = \int_{t_0}^{\infty} P(t_0, \mathbf{z}_0, t - t_0)(t - t_0)^2 dt$$

Example-1: Maximum Growing Maniford of Lorenz System (Nicolis, 1992)

$$\frac{d\xi}{dt} = (\sigma - g\xi^2) + v(t)\xi, \qquad 0 \le \xi < \infty$$

$$\langle v(t) \rangle = 0, \qquad \langle v(t)v(t') \rangle = q^2 \delta(t - t').$$

$$\sigma = 0.64, \qquad g = 0.3, \qquad q^2 = 0.2.$$

Mean and Variance of FPT

$$(\sigma\xi_0 - g\xi_0^2)\frac{d\tau_1}{d\xi_0} + \frac{q^2\xi_0^2}{2}\frac{d^2\tau_1}{d\xi_0^2} = -1$$

$$(\sigma\xi_0 - g\xi_0^2)\frac{d\tau_2}{d\xi_0} + \frac{q^2\xi_0^2}{2}\frac{d^2\tau_2}{d\xi_0^2} = -2\tau_1$$

$$\tau_1 = 0, \qquad \tau_2 = 0 \qquad \text{for} \quad \xi_0 = \varepsilon .$$

$$\frac{d\tau_1}{d\xi_0} = 0, \qquad \frac{d\tau_2}{d\xi_0} = 0 \qquad \text{for} \quad \xi_0 = \xi_{\text{noise}}.$$

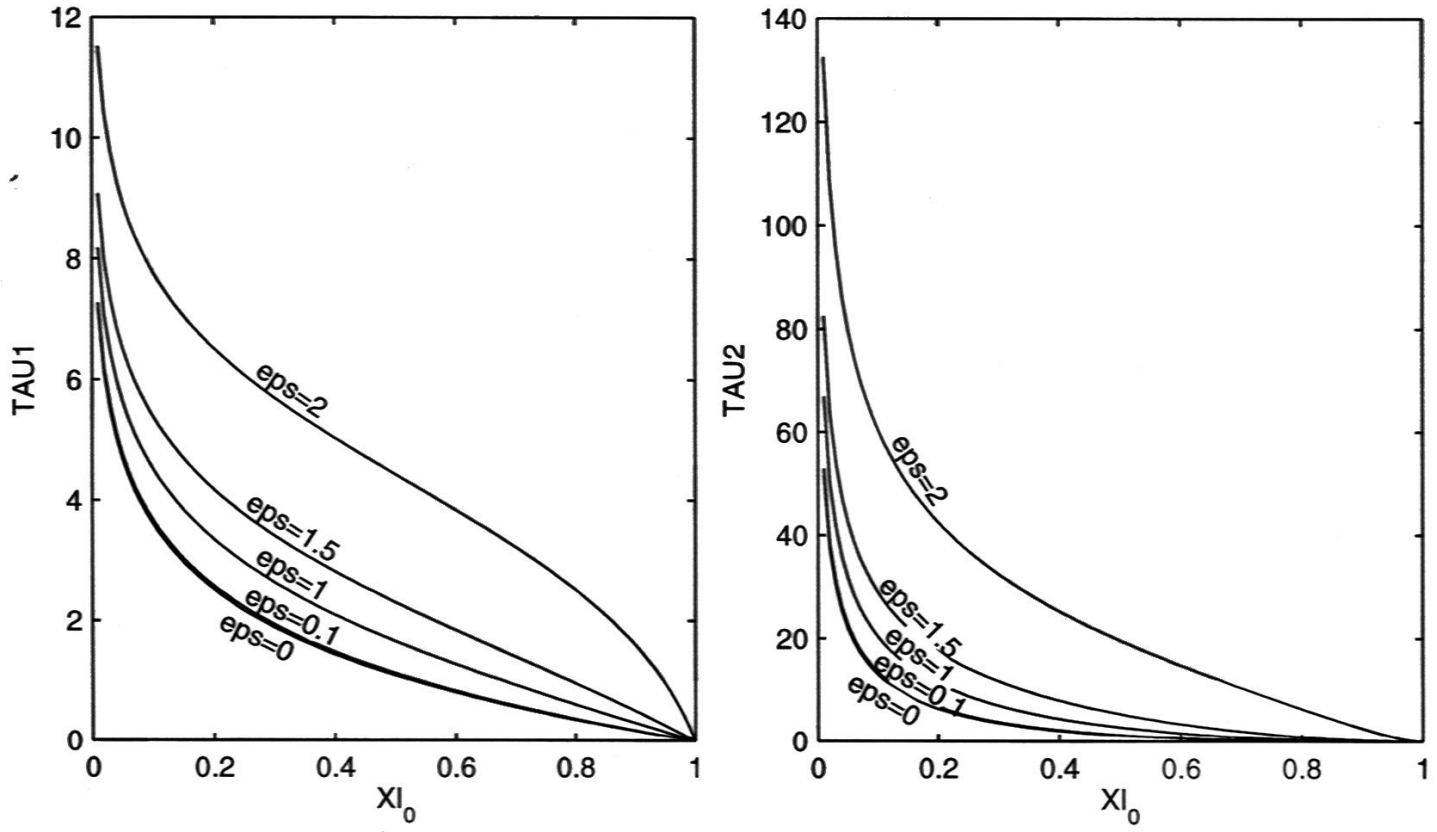
Analytical Solutions

$$\tau_1(\bar{\xi}_0, \bar{\xi}_{noise}, \varepsilon) = \frac{2}{q^2} \int_{\bar{\xi}_0}^{1} y^{-\frac{2\sigma}{q^2}} \exp\left(\frac{2\varepsilon g}{q^2} y\right) \left[\int_{\bar{\xi}_{noise}}^{y} x^{\frac{2\sigma}{q^2}-2} \exp\left(-\frac{2\varepsilon g}{q^2} x\right) dx \right] dy$$

$$\tau_2(\bar{\xi}_0, \bar{\xi}_{noise}, \varepsilon) = \frac{4}{q^2} \int_{\bar{\xi}_0}^{1} y^{-\frac{2\sigma}{q^2}} \exp\left(\frac{2\varepsilon g}{q^2} y\right) \left[\int_{\bar{\xi}_{noise}}^{y} \tau_1(x) x^{\frac{2\sigma}{q^2}-2} \exp\left(-\frac{2\varepsilon g}{q^2} x\right) dx \right] dy$$

$$\bar{\xi}_0 = \xi_0 / \varepsilon, \qquad \bar{\xi}_{noise} = \xi_{noise} / \varepsilon$$

Dependence of tau1 & tau2 on Initial Condition Error (ξ_0/ε)



Example-2: Lorenz System (1984) Modified Hadley Circulation

$$\frac{dx_1}{dt} = -x_2^2 - x_3^2 - ax_1 + aF,$$

$$\frac{dx_2}{dt} = x_1 x_2 - bx_1 x_3 - x_2 + G,$$

$$\frac{dx_3}{dt} = bx_1 x_2 + x_1 x_3 - x_3,$$

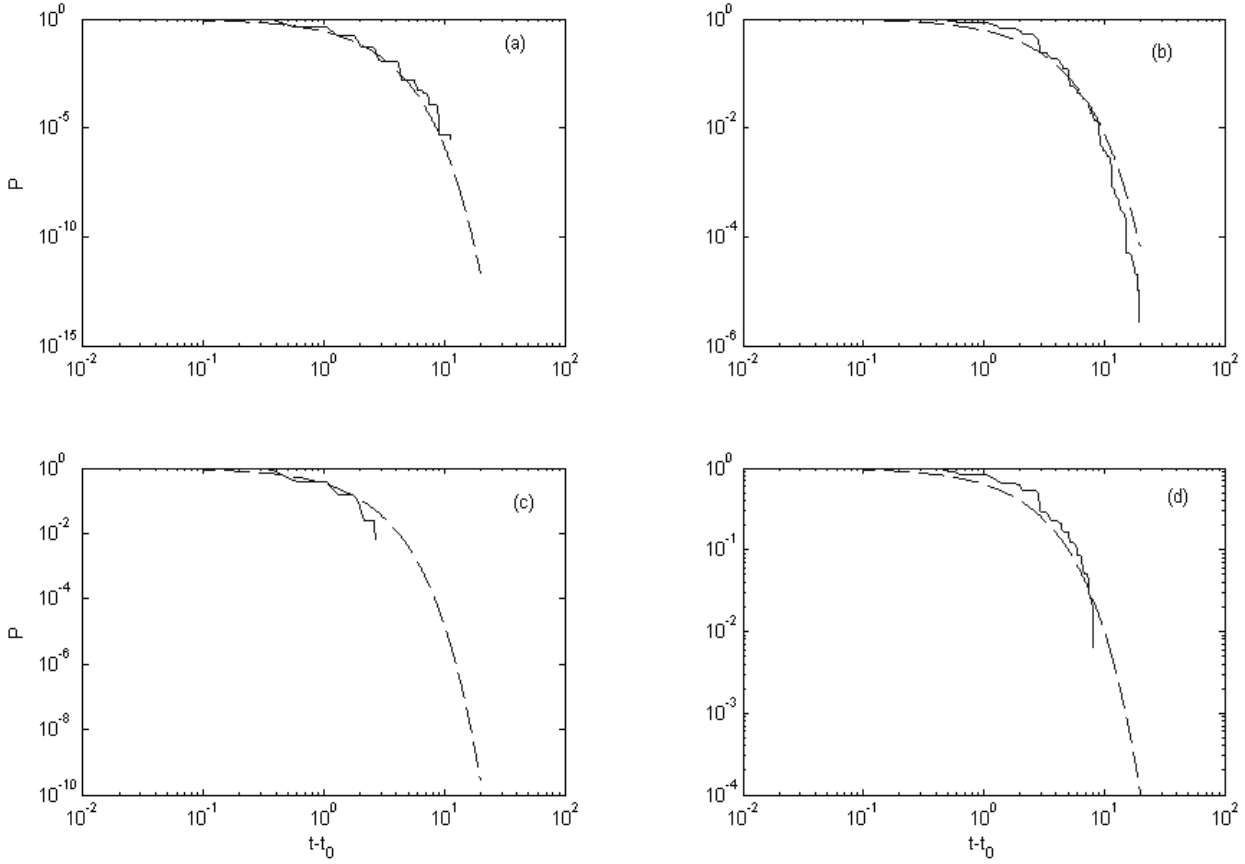
Sensitivity of PDF on the tolerance level and ensemble dimension: numerical (solid curve), analytic (dashed curve)

ε=0.1

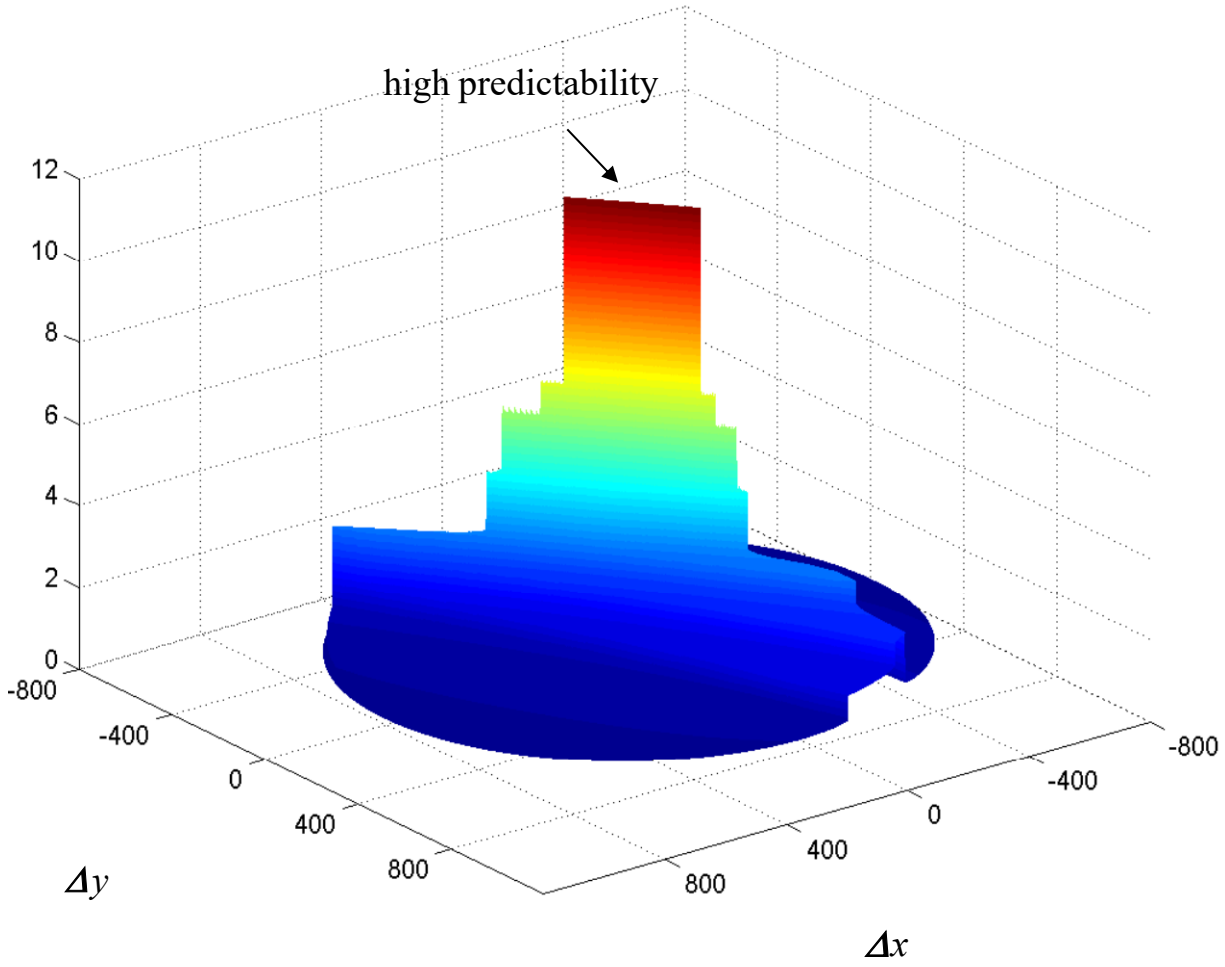
ε=0.5

N=250,000

N=100



Dependence of FPT on Initial Error (Dx, Dy) for $\varepsilon = 0.1$



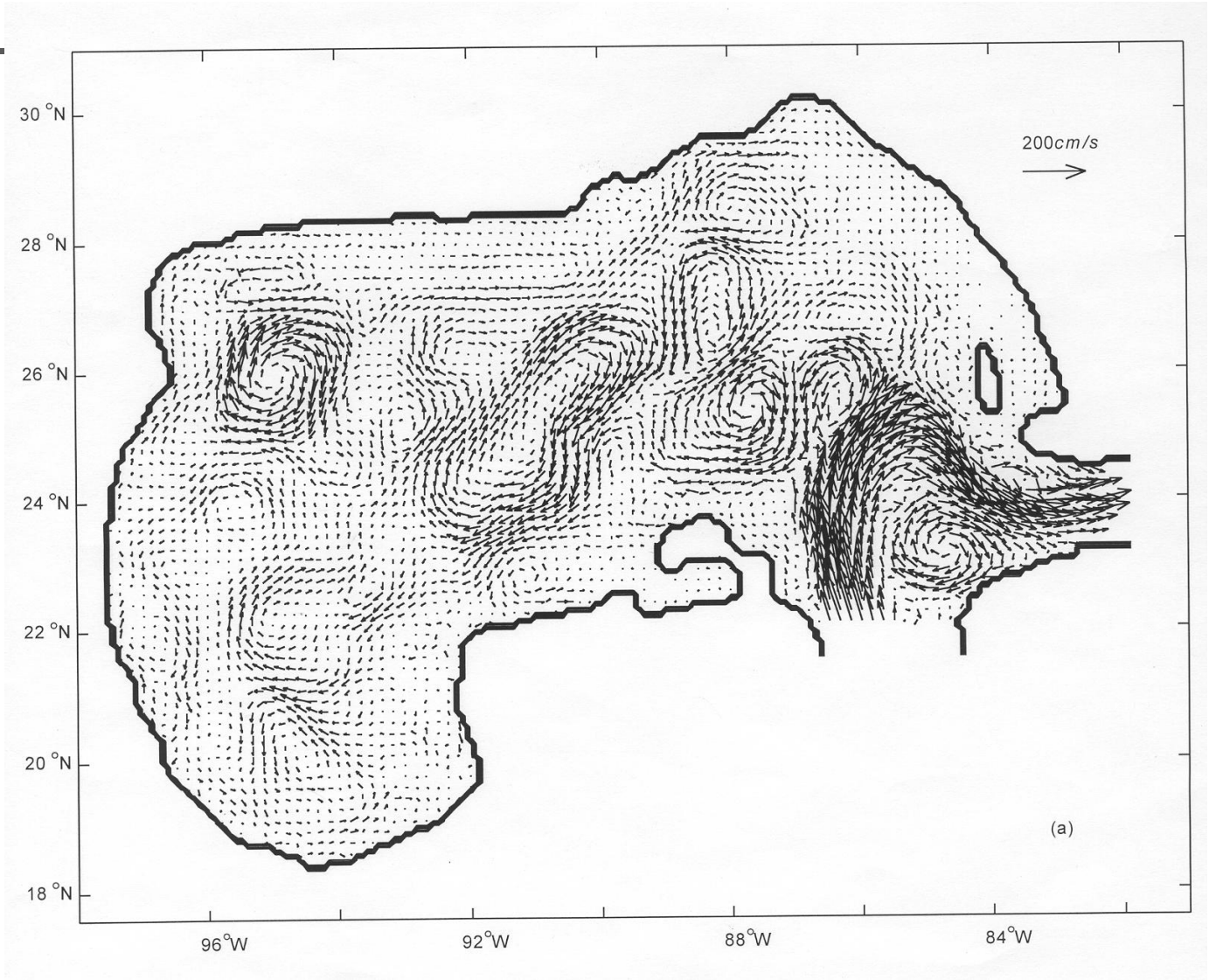
(3) Power Law Decay of Model Predictability Skill

Gulf of Mexico Prediction System

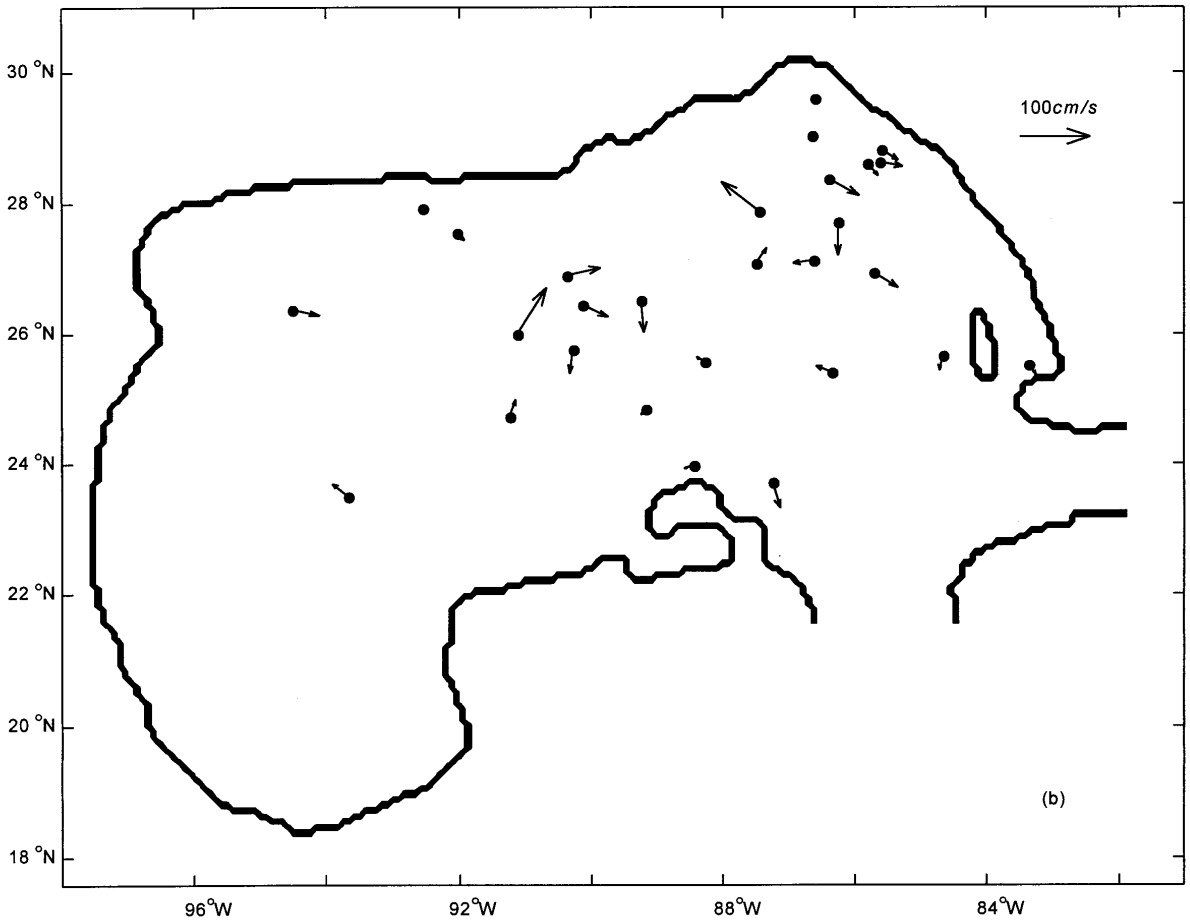
Gulf of Mexico Forecast System

- University of Colorado Version of POM
- 1/12^{o} Resolution
- Real-Time SSH Data (TOPEX, ESA ERS-1/2) Assimilated
- Real Time SST Data (MCSST, NOAA AVHRR) Assimilated
- Six Months Four-Times Daily Data From July 9, 1998 for Verification

Model Generated Velocity Vectors at 50 m on 00:00 July 9, 1998



(Observational) Drifter Data at 50 m on 00:00 July 9, 1998



Error Mean and Variance

Error Mean $$L_1 = \langle \mathbf{z} \rangle$$

Error Variance $$L_2 = \left\langle \left(\mathbf{z} - \langle \mathbf{z} \rangle\right)^t \left(\mathbf{z} - \langle \mathbf{z} \rangle\right) \right\rangle$$

Exponential Error Growth

$$L_1 \propto e^{\sigma t}, \qquad L_2 \propto e^{\omega t},$$

Classical Linear Theory

No Long-Term Predictability

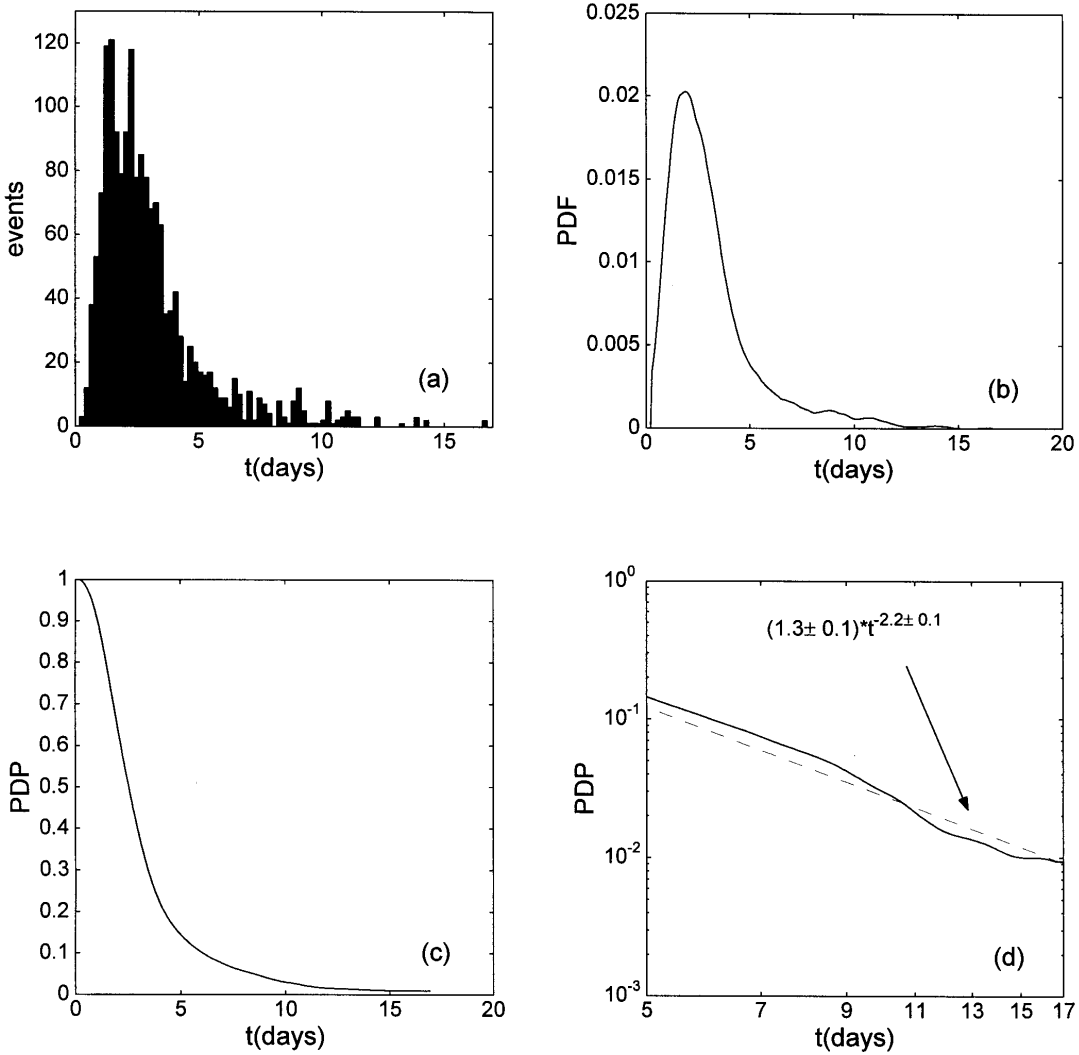
Power Law

$$L_1 \propto t^{\alpha}, \qquad L_2 \propto t^{\beta},$$

$$P(t_0, \mathbf{z}_0, \varepsilon, t - t_0) \sim t^{-\gamma} \quad \text{for large } t.$$

Long-Term Predictability May Occur

Statistical Characteristics of VPP for zero initial error and 22 km tolerance level (Non-Gaussion)

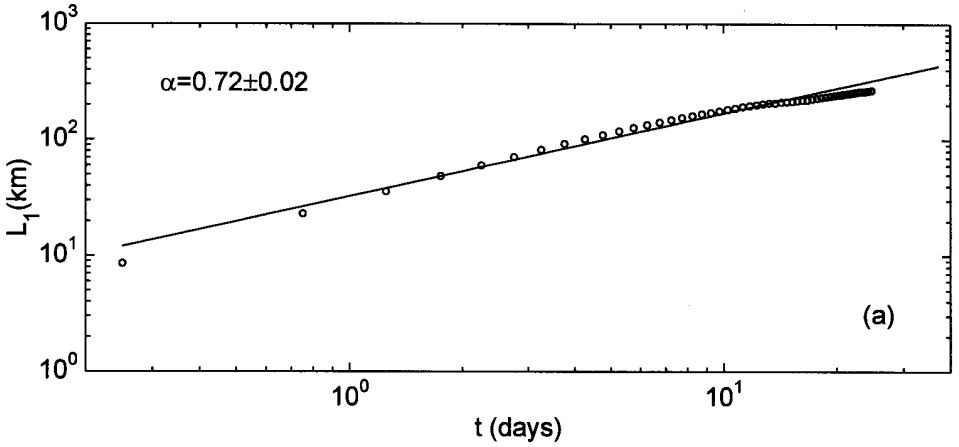


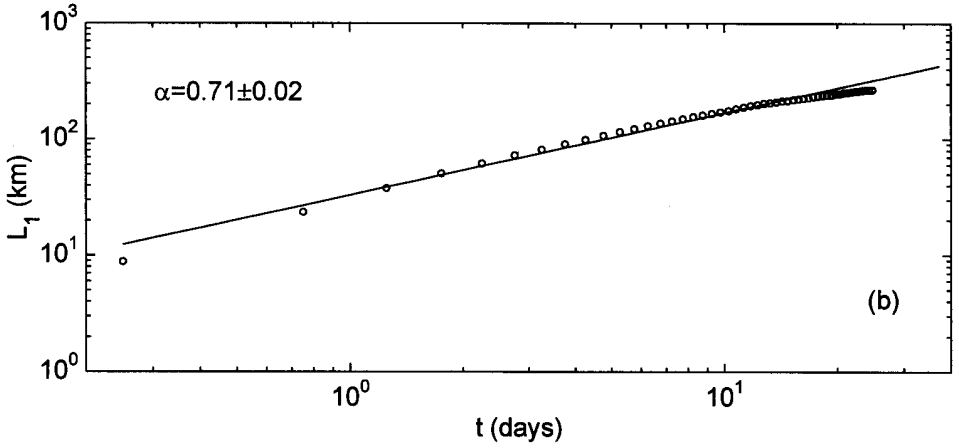
Scaling behavior of the mean error (L_1) growth for initial error levels:

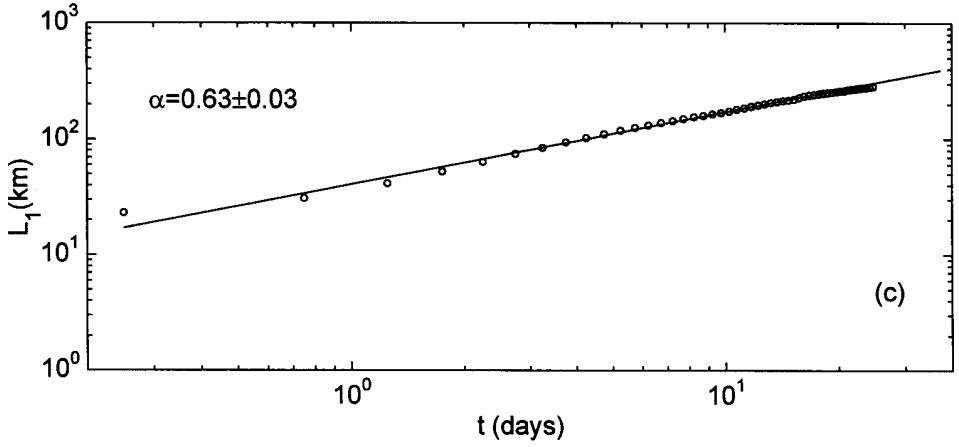
(a) 0

(b) 2.2 km

(c) 22 km







Scaling behavior of the

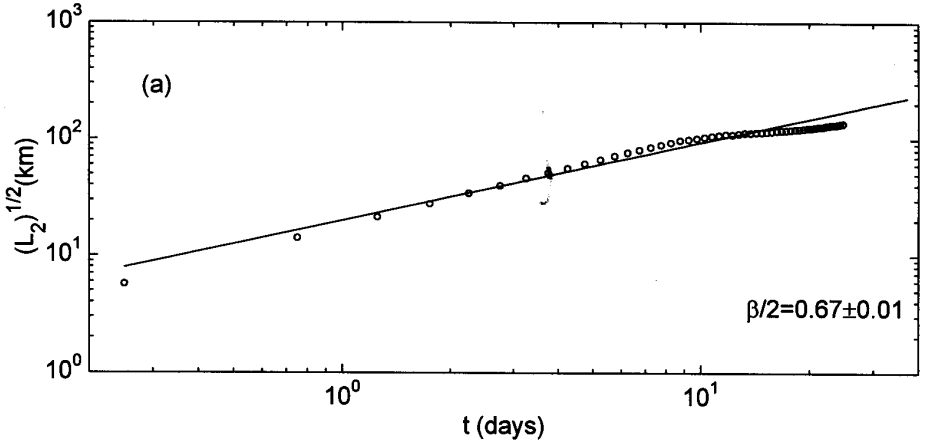
Error variance (L_2) growth

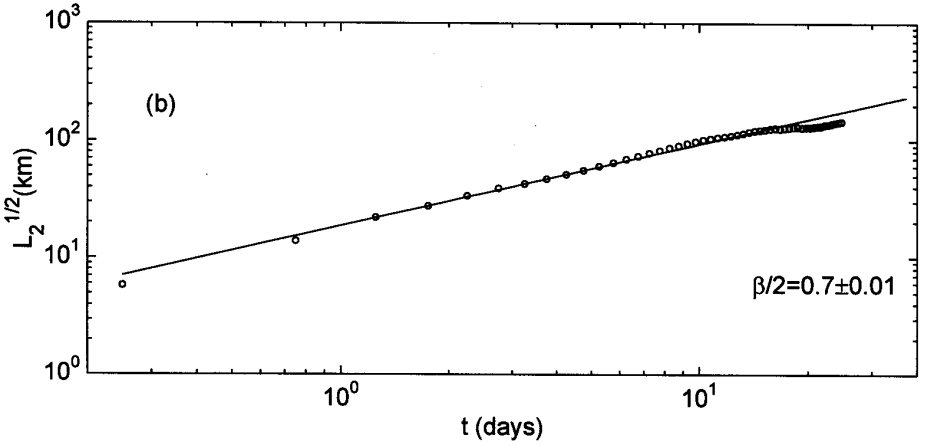
for initial error levels:

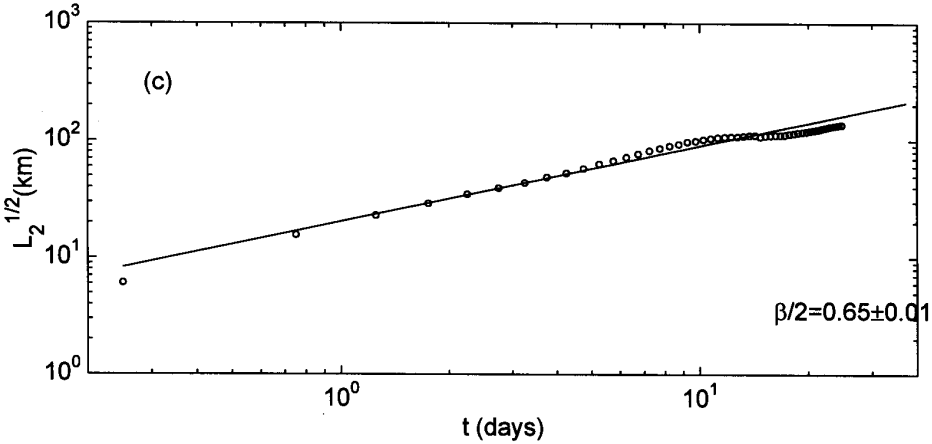
(a) 0

(b) 2.2 km

(c) 22 km

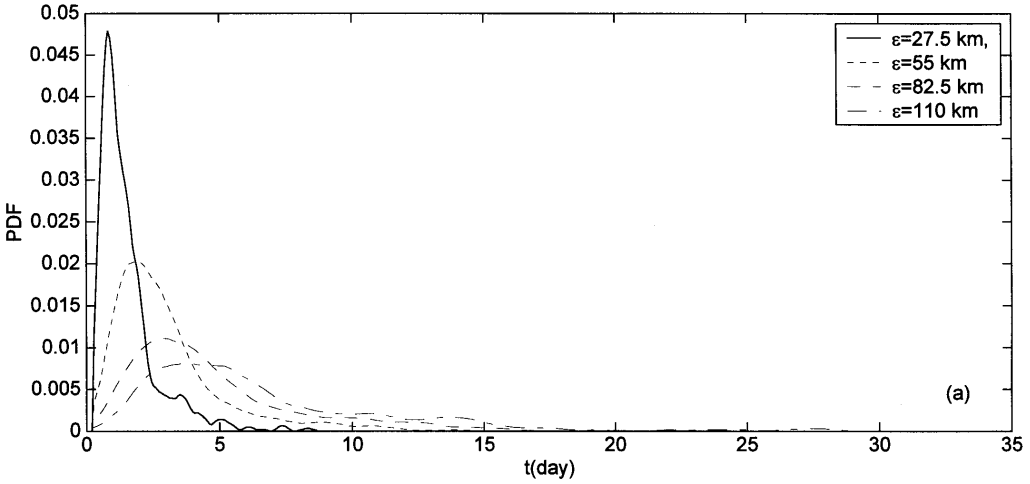


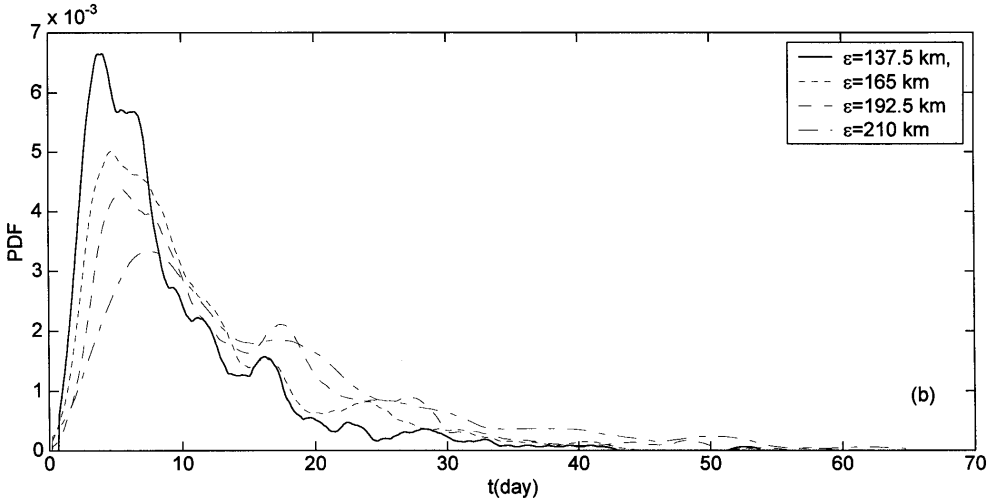


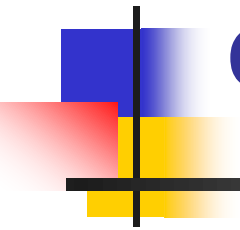


Probability Density Function of VPP calculated with different tolerance levels

Non-Gaussian distribution with long tail toward large values of VPP (Long-term Predictability)







The FPT analysis is usually conducted in the phase space.

Predictability Tube

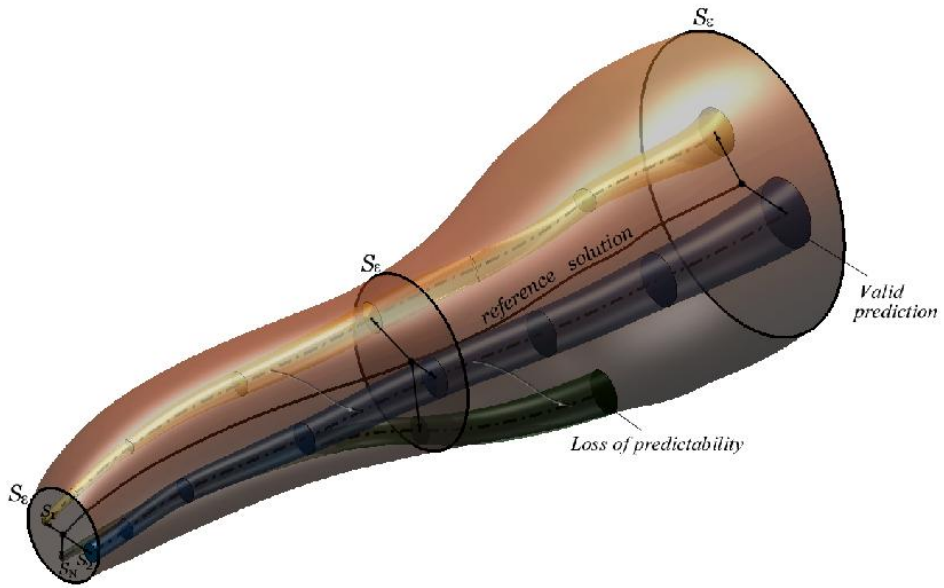


Fig. 31

Conclusions

- OSD is a useful tool for processing real-time velocity data with short duration and limited-area sampling.
- The scheme can handle highly noisy data.
- The scheme is model independent.
- The scheme can be used for velocity data assimilation.
- Phase Space Consideration